JGR Biogeosciences

RESEARCH ARTICLE
10.1029/2019JG005236

Key Points:
- Adsorption to clay selectively removes terrestrial dissolved organic matter (DOM)
- Both DOM composition and water chemistry determine the percentage DOM adsorbed
- The percentage DOM adsorbed was not directly related to water residence time

Supporting Information:
- Figure S1
- Table S1

Correspondence to:
M. Groeneveld,
marloes.groeneveld@ebc.uu.se

Citation:
Groeneveld, M., Catalán, N., Attermeyer, K., Hawkes, J., Einarsdóttir, K., Kothawala, D., et al. (2020). Selective adsorption of terrestrial dissolved organic matter to inorganic surfaces along a boreal inland water continuum. *Journal of Geophysical Research: Biogeosciences*, *125*, e2019JG005236. https://doi.org/10.1029/2019JG005236

Received 4 SEP 2019
Accepted 18 FEB 2020
Accepted article online 28 FEB 2020

Selective Adsorption of Terrestrial Dissolved Organic Matter to Inorganic Surfaces Along a Boreal Inland Water Continuum

Marloes Groeneveld[1], Núria Catalán[2], Katrin Attermeyer[1,4], Jeffrey Hawkes[3], Karólína Einarsdóttir[1], Dolly Kothawala[1], Jonas Bergquist[3], and Lars Tranvik[1]

[1]Department of Ecology and Genetics, Limnology, Uppsala University, Uppsala, Sweden, [2]Catalan Institute for Water Research (ICRA), Girona, Spain, [3]Department of Chemistry—BMC, Analytical Chemistry, Uppsala University, Uppsala, Sweden, [4]WasserCluster Lunz GmbH, Austria

Abstract Different processes contribute to the loss or transformation of dissolved organic matter (DOM) and change DOM concentration and composition systematically along the inland water continuum. Substantial efforts have been made to estimate the importance of microbial and photochemical degradation for DOM concentration and composition and, to some extent, also DOM losses by flocculation, whereas the significance of DOM adsorption to inorganic surfaces has received less attention. Hence, knowledge on the possible extent of adsorption, its effect on DOM loads and composition and on where along the aquatic continuum it might be important, is currently limited or lacking altogether. Here we experimentally determine DOM adsorption onto mineral particles in freshwater ecosystems covering a water residence time gradient in boreal landscape Sweden. We hypothesized that adsorption would gradually decrease with increasing water residence time but actually found that DOM is highly susceptible to adsorption throughout the aquatic continuum. Mass spectrometry and fluorescence analysis on DOM suggest that freshly produced aquatic DOM is less susceptible to adsorption than more terrestrial material. Moreover, the percentage DOM adsorbed in the experiments greatly exceeds the actual adsorption taking place in boreal inland waters across all studied systems. These results illustrate the potential impact of mineral erosion, for example, as a result of agriculture, mining or forestry practices, on the availability, transport, and composition of organic carbon in inland waters.

Plain Language Summary Freshwaters are an important part of the global carbon cycle. They produce organic matter internally and receive large amounts of organic matter from the surrounding land. Within freshwaters, organic matter can be transported to the ocean, converted to carbon dioxide and methane, or buried in the sediment, depending on the chemical composition of the organic molecules and environmental conditions. One pathway toward burial is adsorption onto inorganic particles, such as clay, that may have entered the water by erosion. In this study, we added clay particles to 30 water samples collected throughout Sweden, from peats to very large lakes. We found that a large part of the organic matter could be adsorbed onto the clay and that molecules derived from land-vegetation are more likely to be adsorbed than molecules produced in the water. As a result, adsorption to clay changes the composition of the organic matter in the water. We observed that the potential for adsorption exceeds the adsorption actually taking place in most natural systems. This implies that introduction of minerals by erosion, for example, as a result of agriculture, mining, or forestry practices, could affect the composition of organic matter and thereby its fate in the carbon cycle.

1. Introduction

Organic matter (OM) is continuously transformed and mineralized as it is transported from soils to the ocean (Cole et al., 2007). Mechanisms that are responsible for these changes include microbial degradation, photochemical degradation, flocculation, and adsorption to mineral surfaces. However, the relative contributions of each of these processes to observed changes in dissolved OM (DOM) composition are poorly constrained, as is the spatial distribution of these processes along the aquatic continuum from headwaters to the sea. Substantial efforts have been made to estimate the importance of microbial (Amon & Benner, 1996; Catalán et al., 2016; Fasching et al., 2014) and photochemical degradation (Cory et al., 2014; Koehler

et al., 2014), and to some extent also DOM losses by flocculation (Droppo & Ongley, 1994; Von Wachenfeldt & Tranvik, 2008) and subsequent degradation of these particles (Attermeyer et al., 2018), whereas the role of DOM adsorption to inorganic surfaces for the loss and transportation along the continuum has received limited attention.

The aquatic continuum can be regarded as a gradient of water residence times. Along this gradient, DOM decomposition rates have been found to decrease (Catalán et al., 2016; Evans et al., 2017) and DOM composition varies systematically (Hutchins et al., 2017; Kellerman et al., 2014; Lambert et al., 2016). Roughly half of the terrestrially derived organic matter is lost during transport through the aquatic continuum (Algesten et al., 2003). The removal of terrestrial OM has been attributed to a combination of photodegradation and biodegradation in various systems (Chen & Jaffé, 2014; Seidel et al., 2015; Weyhenmeyer et al., 2012). Furthermore, adsorption of DOM has been put forward as another potential removal process for terrestrial DOM (Seidel et al., 2015), but so far, we lack studies that systematically investigate the potential and qualitative effects of adsorption on the DOM pool across a variety of inland waters.

Adsorption is a physicochemical process that can stabilize OM to a solid surface, potentially preventing, or postponing, degradation by protecting it from enzymatic decay (e.g., Hunter et al., 2016; Kaiser & Guggenberger, 2000; Kalbitz et al., 2005). The extent to which adsorption occurs depends on the nature of the sorbent (i.e., the inorganic particles), the sorbate (i.e., the OM compounds), and water chemistry characteristics such as pH and ionic strength (Sollins et al., 1996). Certain components of the sorbent make it more or less prone to attract organic compounds, for instance, aluminum and iron oxides and hydroxides may engage in adsorptive processes, where the hydroxyl ligand group is traded for a negatively charged OM compound via ligand exchange (Kaiser et al., 1996; McKnight et al., 1992; Tipping, 1981a; Yoon et al., 2004). As for the sorbate, hydrophobic compounds are more prone to leave solution (Kleber & Johnson, 2010), and carboxylic and hydroxylic groups allow for ligand exchange with metals on mineral surfaces (Kaiser et al., 1996). In general, aromatic molecules with many functional groups are particularly likely to adsorb to mineral surfaces (Kalbitz et al., 2005; Kleber et al., 2015). Accordingly, OM quality analyses through spectroscopic characteristics and isotopes have shown that complex, aromatic compounds are preferentially adsorbed, while aliphatic compounds with few functional groups (particularly carboxylic and hydroxylic groups) bind less strongly to the mineral soil and thus turn over quicker (Gu et al., 1994; Kalbitz et al., 2005; Kothawala et al., 2012). Furthermore, cation bridges can form between negatively charged clay and OM compounds (Ahmed et al., 2002; Theng, 1976) and high ionic strength can increase OM adsorption by masking the negative charges and decreasing the repulsive forces between and within OM molecules, allowing them to assemble more compactly on the sorbent (Shen, 1999). Low pH has a similar effect of masking negative charges on DOM by protonation, decreasing its solubility and enhancing its affinity for mineral surfaces (Kaiser et al., 1996). Accordingly, adsorption has been found to decrease with increasing pH for OM fractions extracted from lake water (Gu et al., 1994; Shen, 1999) and soils (Fleury et al., 2017; Kaiser et al., 1996; Shen, 1999). These results suggest that water chemistry plays an important role in determining the quantity and quality of DOM adsorbed onto mineral particles, which has not been assessed across a gradient of naturally occurring DOM.

Adsorption has been extensively studied in soils (e.g., Kaiser et al., 1996; Kaiser & Guggenberger, 2000; Kalbitz et al., 2005) where it helps determine whether OM can be flushed out in runoff and reach the aquatic system. Furthermore, the role of adsorption is well studied in estuaries (Hedges & Keil, 1999; Tremblay & Gagné, 2009), where it has for example been found to remove 6%–62% of the colored riverine DOM within 30 km off shore (Uher et al., 2001) and, in marine sediments (e.g., Keil et al., 1994; Mayer, 1994a), where the OM to inorganic surface ratio is low, and the available surface area controls the amount of adsorption (Mayer, 1994b). In surface waters, adsorption to suspended particles may intercept OM and prevents it from being transported to the ocean or transformed by other processes. However, the importance and effect of adsorption on DOM composition and stabilization in inland waters has not been studied comparatively across freshwater systems. Earlier studies have only considered up to four sites at a time and worked in most cases with specific fractions of the DOM pool (e.g., Day et al., 1994; Gu et al., 1995; Luider et al., 2003; Meier et al., 1999; Tipping, 1981b). Although inorganic surfaces are assumed to be in low supply in pristine aquatic systems, this is not always the case. Certain land uses, such as agriculture and forestry, as well as flooding events, may lead to increased load of suspended solids (Syvitski et al., 2005; Walling & Fang, 2003), and

certain water chemistry parameters, such as low pH and the presence of cations, may provide a favorable setting for adsorption to occur.

To address the role of adsorption for the loss and transformation of DOM in inland waters, this study aims to explore the adsorption potential for DOM in the boreal inland water continuum, which typically exhibits high concentrations of DOM (Sobek et al., 2007) and where about half of the dissolved organic carbon (DOC) imported from terrestrial habitats is lost during transport to the sea (Algesten et al., 2003). Building on the findings of changing DOM with increasing water residence time (WRT; Kellerman et al., 2014; Lambert et al., 2016; Hutchins et al., 2017), we investigated the quantitative (i.e., the amount and proportion of DOM that is adsorbed) and qualitative importance of adsorption (i.e., the change in DOM composition as a result of adsorptive processes) along a WRT gradient. Since the sampled systems contain substantial natural diversity in DOM composition and water chemistry, we additionally aim to uncover which DOM quality and water chemistry parameters affect adsorption on a landscape scale. Therefore, we assessed DOM adsorption to mineral surfaces across 30 boreal systems, covering a WRT gradient from peat surface water as the terrestrial endmember through streams and lakes to a maximum residence time of 60 years. We hypothesized that the potential for adsorption is gradually exhausted along the aquatic continuum with increasing WRT, as the proportion of terrestrial DOM decreases over time.

2. Materials and Methods

2.1. Water Sampling and In Situ Measurements

Water samples were collected between 28 August and 6 September 2016 from 20 lakes, three peats and seven streams and rivers throughout Sweden, covering the regions of Jämtland, Bergslagen, Uppland, and Småland (Figure 1 and Table 1). Lake water was collected at 0.5-m depth with a Ruttner sampler. Grab samples were taken from the surface of shallow streams and water filled depressions of peat bogs, except for one peat (site 10), where a hole was made in the peat to collect a sufficient amount of water. Temperature, oxygen and conductivity (HQ40d, Hach, Loveland, Colorado, USA), and pH (Hanna HI991300; Woonsocket, Rhode Island, USA) were measured in situ. Water samples were filtered (precombusted Whatman GF/F, approximate pore size 0.7 μm) into acid-washed and combusted (450 °C for 4 hr) glass bottles upon return to the laboratory (within 72 hr) and stored in the dark at 4 °C until further analysis.

2.2. Water Residence Time Calculations

We defined WRT as the ratio of the mass of water in a particular water body to the rate of renewal of that water (Monsen et al., 2002). For lakes, WRT was calculated as the volume of the lake (V; m^3) divided by water inputs (total Q) as obtained from previous studies (see Table 1). In streams and rivers, WRT is defined as the length of the stream reach (L; m) divided by water mean velocity (v; m/s). Discharge was measured in streams and smaller rivers during the sampling campaign. For the small headwater stream (site 8), discharge (Q; l/s) and v were determined through slug addition of 1 L NaCl enriched solution (Gordon et al., 2004). In the case of sites 16, 22, and 24, a current meter (μP-TAD, Höntzsch Instruments, Waiblingen, Germany) was used to obtain Q and v. In the case of sites 17 and 28, discharge could not be measured in the field due to the high flow conditions and site 26 data was lost. In these cases, the interface HYPE from the Swedish meteorological and Hydrological institute (http://vattenwebb.smhi.se/modelarea/; 14 November 2017) was used to obtain mean Q during the month preceding the sampling date and v was obtained from the cross-sectional area. The total area of the catchment was also obtained from the HYPE database for all the streams and rivers. For site 8, with a known reach length and velocity and not included in HYPE, we obtained WRT as L/v. In the other cases, we obtained the length of catchment upstream (L_c), assuming it had the height of an isosceles triangle with known area, obtaining similar values as Raymond et al. (2016) for similar stream orders. WRT was then obtained as L_c/v, resulting in WRT's typical for boreal systems (see Weyhenmeyer et al., 2012). As the calculated WRT's for running waters are subject to errors associated with each of the three methods used, we compare these results with stream order, which should approximate WRT. Strahler stream order was obtained from a virtual stream network of Sweden (VIVAN), which is based on a digital elevation model (50 × 50 m resolution) in combination with hydrographical information from the national roadmap (scale 1:100 000), established catchment borders and mean discharge during base flow (Nisell et al., 2007). Data analyses were performed with both calculated WRT and Strahler stream order and lead to highly similar results (supporting information (SI) Text S1 and Figure S1).

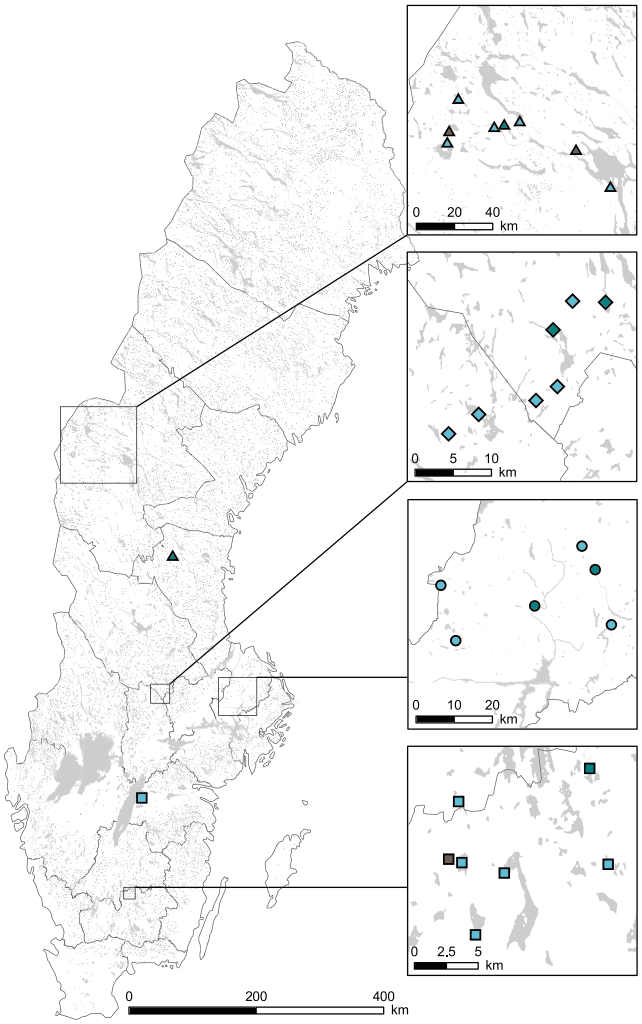

Figure 1. Map of Sweden with sampling sites in Jämtland [triangles], Bergslagen [diamonds], Uppland [circles], and Småland [squares]: lakes (blue), streams (green), and peat waters (brown).

2.3. Batch Adsorption Experiments

Batch experiments were performed in triplicate by exposing water samples from the 30 aquatic ecosystems described above to the reference material "IPT.32 Plastic Clay" (51.8% SiO_2, 28.5% Al_2O_3, 3.46% Fe_2O_3, 1.49% TiO_2, <1% K_2O, MgO, CaO, Na_2O, and P_2O_5, Bureau of Analysed Standards LTD, Middlesbrough, UK). The clay originates from an alluvium consisting of fluvial, marine, and aeolian deposits and is composed of approximately 80% kaolinite, 10% quartz, 5% illite, 5% feldspar, and a trace of smectite (Hosterman et al., 1987) and was chosen for its ability to adsorb DOM (SI Text S2). The water samples (300 ml) were refiltered (Whatman GF/F) into acid-washed and combusted (450 °C for 4 hr) 300 ml glass bottles. After initial samples were taken (200 ml remaining), 1 g of "IPT.32 Plastic Clay" mineral clay was added to each triplicate. The mineral clay was prewashed twice with MQ before addition to minimize desorption of material during the incubations. Subsequently, the clay was dried at 110 °C for 2 hr and added to the bottles as a powder at a concentration of 5 g L^{-1} as this is substantially higher than naturally occurring levels in waters in this region (data only available for Uppland, range: 0–290 mg L^{-1}, median: 10 mg L^{-1}; http://info1.ma.slu.se/). Consequently, we experimentally evaluated the fraction of DOM adsorbed (as a percentage) at the set concentration of mineral particles. The samples were stirred with a magnetic rod for 20 hr in the dark at 13 °C to allow for an equilibrium to be reached while minimizing microbial degradation (e.g., Kaiser et al., 1996; Meier et al., 1999). A mixing time of 20 hr was considered to be sufficient to reach equilibrium, since

Table 1
Sampling Sites and Environmental Data

ID	Name	Region	Type	WRT (year)	pH	Conductivity ($\mu S\ cm^{-1}$)	DOC ($mg\ L^{-1}$)	TN ($mg\ L^{-1}$)	TP ($\mu g\ L^{-1}$)	Chl*a* ($\mu g\ L^{-1}$)	A_{420} (m^{-1})
1	Vättern	Småland	lake	60[a]	8.3	147	2.9	0.56	4.4	0.36	0.14
2	Skärshultsjön	Småland	lake	0.12[b]	6.5	50	15.1	0.58	15.7	1.54	5.18
3	Förhultasjön	Småland	lake	0.72[b]	7.3	57	11.3	0.45	8.4	2.10	1.97
4	Aneboda	Småland	peat	NA	4.8	44	29.3	0.97	35.2	3.83	12.62
5	Fiolen	Småland	lake	6.5[b]	7.1	50	7.1	0.43	11.4	2.71	0.80
6	Stråken	Småland	lake	10.7[b]	6.8	61	10.8	0.44	11.4	2.92	2.08
7	Klintsjön	Småland	lake	4.7[c]	5.9	38	4.1	0.25	5.5	0.98	0.37
8	Hisshult	Småland	stream	$3.1{\cdot}10^{-5}$[d]	5.9	100	22.1	1.15	46.3	29.15	9.18
9	Storsjön	Jämtland	lake	2.0[e]	7.5	44	3.3	0.21	3.1	0.68	0.60
10	Rismyren	Jämtland	peat	NA	6.2	NA	31.2	2.84	179.7	3.70	8.66
11	Ånnsjön	Jämtland	lake	1.1[e]	7.8	56	3.5	0.19	6.8	0.54	0.86
12	Duved	Jämtland	peat	NA	5.8	44	36.3	0.75	26.1	1.76	7.94
13	Häggsjön	Jämtland	lake	$3.2{\cdot}10^{-2}$[b]	7.3	37	4.3	0.17	3.1	0.61	0.97
14	Kallsjön	Jämtland	lake	2.3[e]	7.4	29	3.0	0.23	6.3	0.09	0.47
15	Åresjön	Jämtland	lake	$2.8{\cdot}10^{-2}$[e]	7.8	40	2.9	0.16	3.2	0.52	0.32
16	Linan	Jämtland	stream	$8.7{\cdot}10^{-4}$[f]	7.7	32	2.6	0.11	1.1	0.19	0.51
17	Ljusnan	Jämtland	river	$3.0{\cdot}10^{-3}$[g]	7.8	31	6.7	0.21	5.0	1.20	2.41
18	Gäddtjärn	Bergslagen	lake	0.26[c]	7.6	65	10.6	0.30	9.3	0.59	4.44
19	Svarttjärn	Bergslagen	lake	$4.0{\cdot}10^{-2}$[c]	6.0	71	15.3	0.28	13.8	1.30	5.65
20	Lilla Sångaren	Bergslagen	lake	1.2[c]	7.3	47	6.4	0.26	6.0	0.96	1.46
21	Ljustjärn	Bergslagen	lake	4.3[c]	7.3	22	3.2	0.23	7.6	0.59	0.43
22	Hedströmmen	Bergslagen	stream	$2.8{\cdot}10^{-3}$[f]	6.8	22	8.3	0.26	6.8	0.79	2.21
23	Oppsveten	Bergslagen	lake	0.43[e]	6.7	27	16.2	0.41	8.1	2.41	5.82
24	Bjursjöbacken	Bergslagen	stream	$1.4{\cdot}10^{-2}$[f]	7.1	37	12.6	0.39	12.2	0.96	3.52
25	Lötsjön	Uppland	lake	4.4[h]	8.2	212	11.3	1.12	24.8	15.28	0.52
26	Sävjaån	Uppland	stream	$6.8{\cdot}10^{-3}$[g]	7.2	279	22.6	1.07	77.3	0.67	5.87
27	Stensjön	Uppland	lake	$5.5{\cdot}10^{-2}$[h]	7.2	162	18.6	0.76	20.3	3.07	4.71
28	Fyrisån	Uppland	river	$6.2{\cdot}10^{-3}$[g]	7.8	384	16.5	1.10	39.8	1.15	2.05
29	Siggeforasjön	Uppland	lake	0.49[h]	7.2	44	15.5	0.51	9.3	0.81	4.11
30	Ramsjön	Uppland	lake	1.4[e]	7.5	109	23.8	0.76	29.1	2.78	7.70

Note: (a) Lindell et al. (2001), (b) unpublished data, (c) von Wachenfeldt and Tranvik (2008), (d) calculated based on slug addition, (e) calculated from data http://vattenweb.smhi.se, (f) currentimeter, (g) based on HYPE, and (h) Brunberg and Blomqvist (1998). WRT = water residence time, DOC = dissolved organic carbon, TN = total nitrogen, TP = total phosphorus, Chl*a* = chlorophyll *a*, A_{420} = absorbance at 420 nm.

adsorption is a physical process that takes place on a time scale from minutes to hours (Lv et al., 2016; Meier et al., 1999). After the incubation, the samples were centrifuged for 45 min at 9000 RCF and the supernatant was filtered (Whatman GF/F, approximate pore size 0.7 μm). Final samples were taken from the filtrate. DOC concentrations, DOM composition (Orbitrap mass spectrometry), absorbance, and fluorescence scans were determined before and after exposure to the clay. Conductivity, total suspended solids (TSSs) and pH were measured with a multiparameter probe (Hanna HI-991300; Woonsocket, Rhode Island, USA).

2.4. Water Chemistry

DOC concentrations were determined using a Sievers M9 total organic carbon (TOC) analyzer (GE Analytical Instruments, Boulder, Colorado, USA). Total nitrogen (TN) concentrations were determined on a TOC/TN analyzer (Shimadzu TOC-L/TNM-L, Kyoto, Japan). Total phosphorus concentrations were measured colorimetrically with a UV/Vis spectrophotometer (Lambda 40; Perkin Elmer; Waltham, Massachusetts, USA) using the molybdenum-blue method (Menzel & Corwin, 1965).

Anions and cations were measured on samples filtered over prerinsed 0.2-μm Acrodisc Supor hydrophilic polyethersulfone membranes (Pall Laboratory, Port Washington, New York, USA) and stored frozen. Anions (F^-, Cl^-, NO_3^-, PO_4^{3-}, and SO_4^{2-}) were separated on a Metrosep A Supp 5 analytical column (150 × 4.0 mm) fitted with a Metrosep A Supp 4/5 guard column at 0.7 ml min^{-1} using a carbonate eluent (3.2 mM Na_2CO_3 + 1.0 mM $NaHCO_3$). Cations (Na^+, NH^+, K^+, Ca^{2+}, and Mg^{2+}) were separated on a Metrosep C4 column (250 × 2.0 mm) with a Metrosep C4 guard column with an eluent of 1.7 mM nitric

acid and 0.7 mM dipicolinic acid and a flow rate of 0.2 ml min^{-1}. The analyses were conducted on a Metrohm IC system (883 Basic IC Plus and 919 Autosampler Plus).

Chlorophyll *a* was determined from suspended material collected on precombusted filters (Whatman GF/F, approximate pore size 0.7 μm), which were stored at −20 °C after filtration. The Chl *a* was dissolved in ethanol for 5 min at 75 °C. Subsequently, the Chl *a* concentrations were determined spectrophotometrically (UV/Vis spectrophotometer Lambda 40; Perkin Elmer; Waltham, Massachusetts, USA) following standard guidelines (ISO10260:, 1992; Jespersen & Christoffersen, 1987).

The particulate organic C (POC) and N (PN) contents were analyzed on an Elemental Combustion System (Costech Instruments, Cernusco s/Nav., Italy). The filters were freeze dried prior to analysis and subsequently acidified with 3% HCl in order to eliminate any particulate inorganic carbon (Nieuwenhuize et al., 1994). Thus, the POC/PN ratio is used as an approximation of the commonly used C/N ratio.

2.5. Absorbance and Fluorescence Spectrometry

UV–Vis absorbance spectra (250 to 600 nm) of filtered water were measured in a 0.5 (if $A_{200} > 2$) or 1-cm quartz cuvette using a Lambda35 UV–Vis Spectrometer (PerkinElmer Lambda 25, Perkin Elmer, Waltham, USA). The specific UV absorption coefficient at 254 nm ($SUVA_{254}$; L mg C^{-1} m^{-1}), a proxy for aromaticity (Weishaar et al., 2003), was calculated as the ratio between A_{254} and the DOC concentration (mg C L^{-1}). The 250/365 absorbance ratio was used as a proxy for nonaromatic and low molecular weight compounds (Peuravuori & Pihlaja, 1997), where high values indicate a low degree of aromaticity and low molecular weight, and low values denote a high degree of aromaticity and high molecular weight. Synchronous fluorescence scans were obtained using a FluoroMax-4 Spectrofluorometer (FluoroMax-4, Jobin Yvon, Horiba, Kyoto, Japan), with excitation-emission matrices (EEMs) from excitation wavelengths 250 to 445 nm with 5-nm increments and emission wavelengths 300 to 600 nm with 4-nm increments. The EEMs were blank subtracted using a sample of Milli-Q water run on the same day, corrected for instrument biases and inner filter effects, and normalized to Raman units (Kothawala et al., 2013; Lawaetz & Stedmon, 2009). A shift in the location of the maximum intensity of peak A and peak C was observed across the initial samples and as a result of the adsorption treatment. These locations were determined within Ex_{250}-$Em_{350–500}$ for peak A and $Ex_{300–400}$-$Em_{392–500}$ for peak C. Three commonly used indices were calculated at fixed excitation/emission wavelength pairs or regions: the fluorescence index (FI; Cory & McKnight, 2005), the humification index (Ohno, 2002), and the freshness index (FRESH; Parlanti et al., 2000). All fluorescence corrections were performed using the FDOMcorr toolbox (Murphy et al., 2010) for MATLAB (Mathworks, Inc., Natick, MA).

2.6. Mass Spectrometry

DOM composition was measured by direct infusion electrospray ionization (ESI) Orbitrap mass spectrometry (Fleury et al., 2017; Hawkes et al., 2016). Solid phase extraction was performed with 100-mg Bond Elut PPL cartridges (Agilent Technologies) within 12 days of the adsorption experiment. The cartridges were cleaned once with methanol, allowed to soak in fresh methanol for at least 2 hr, and then rinsed with 0.1% formic acid. The samples were acidified to pH ≈ 2 with 6 M high purity HCl (Suprapure, VWR; 1 μl ml^{-1}) and allowed to flow through the cartridges by gravity. We chose to extract a fixed amount (112 μg C) of organic carbon (as opposed to a fixed volume) in the solid phase extraction step with the aim of studying compositional changes in the DOM after adsorption to clay particles. The cartridges were flushed with 3 ml 0.1% formic acid to remove salts and then dried using N_2. The samples were then eluted with 1ml methanol in precombusted 2-ml amber vials and stored at −20 °C until analysis. We were able to determine the extraction efficiencies for 25 out of 30 sample pairs (before and after adsorption treatment), which ranged from 35% to 95% (mean and median: 61%) with no systematic treatment effect ($p = 0.52$, paired sample *t* test). Samples were diluted to 30 ppm C in 50% methanol and loaded by autosampler (Agilent 1100) in 50-μl aliquots to the Orbitrap mass spectrometer (Velos Pro, Thermo Fisher). A mobile phase of 50% methanol (10 μl min^{-1}) was used to transport the loaded organic material. The ESI source was operated in negative mode at 3 kV and masses were calibrated using the lock mass setting on masses 269.06676, 369.08272, and 425.108935, which were present in every sample. The 150 scans were acquired (4.5 min) for each sample after 3 min, after which lines were flushed for 4.5 min with methanol so that a baseline signal was achieved. Noise was removed and formulas assigned according to in-house routines (Hawkes et al.,

2016), allowing up to $C_{50}H_{100}O_{40}N_1S_1$ under the conditions $150 > m/z > 800$, $0.3 \geq H/C \leq 2.2$, $O/C \leq 1$, and $N + S + {}^{13}C \leq 1$. Formulas were only assigned with a mass error < 0.66 ppm ($1 \times 10^6 \times \Delta m/(m/z)$). Isotopologues ($^{13}C$ peaks) and rare cases of double assignments were removed from consideration. Samples were run in duplicate and only the average peak intensity of formulas that occurred in both replicates were used in the data analysis.

2.7. Data Analyses

Linear relationships were analyzed using Siegel repeated medians linear regressions (Siegel, 1982) since the data were not normally distributed. Peat bog waters were not included in the regressions between fluorescence peak maxima and WRT as we consider them to be at the start of the aquatic continuum and thus did not assign them a value for WRT. WRT was log transformed for all analyses. Wilcoxon signed rank tests for paired samples were used to assess the significance of the shifts in the position of peaks A and C when comparing the fluorescence scans before and after the adsorption treatment. The Kruskall-Wallis test was used in combination with Dunn's test of multiple comparisons using rank sums to determine differences between parallel factor analysis (PARAFAC) components.

In order to determine the effect of adsorption to clay on DOM composition, we first performed a principal coordinate analysis (PCoA) on the Bray-Curtis dissimilarity matrix of the normalized molecular data and determined the correlations between the principal coordinates and additional sample characteristics. It should be noted here that only a limited set of explanatory variables (treatment, DOC, pH, conductivity, A_{254}, and A_{420}) was available for both the start and the end samples and thus the suite of environmental variables that could potentially explain the differences between the samples is by no means complete.

Univariate relationships between FT-Orbitrap-MS peak intensities and WRT and PCoA1, respectively, were analyzed using Spearman correlations and plotted in van Krevelen space (H/C vs. O/C ratio). The correlation limit was set at 0.362 for the correlations with WRT (30 samples, $\alpha = 0.05$) and 0.255 for the correlations with PCoA1 (60 samples, $\alpha = 0.05$).

The effect of adsorption on DOM composition was furthermore studied in van Krevelen space for all individual samples. While we cannot follow the concentrations of individual DOM compounds as approximated by their intensity (overall DOC concentration decreases with adsorption and compounds that were not very abundant before may after adsorption seem relatively more abundant), we can look at which compounds were present before but are absent after treatment, which gives a conservative impression of which compounds are adsorbed. This information was then summarized in terms of H/C and O/C ratios. Weight-averaged H/C ratios (HC_{WA}) were calculated for all samples before and after treatment as follows:

$$HC_{WA} = \sum_{i=1}^{n} \frac{H}{C} * I / \sum_{i=1}^{n} I \tag{2}$$

where H is the number of hydrogen atoms and C is the number of carbon atoms in molecular formula i, I is the intensity of formula i, and n is the total number of formulae in each sample (Hawkes et al., 2018). Weight-averaged O/C ratios (OC_{WA}) were calculated in the same manner.

PARAFAC (Bro, 1997) was used to identify the main fluorescence components of DOM present throughout the samples. The analysis was conducted on a set of 180 samples (30 sites, triplicates, two time points) using the drEEM toolbox for MATLAB (Mathworks, Inc., Natick, MA) following Murphy et al. (2013). EEMs were preprocessed as follows: (1) In three samples, faulty parts were removed from the EEMs, (2) primary and secondary Rayleigh and Raman were removed and smoothed over, and (3) the data were normalized to total fluorescence intensity of each sample. Nonnegativity constraints were applied on all modes (excitation, emission, and sample). The appropriate number of components was identified considering the effect of adding more components on the model fit (expressed as the sum of square errors), by visual inspection of the residuals and random initialization with 20 iterations with a convergence criterion of 1×10^{-08} to find a stable model. The model was validated using random split-half analysis. The components were compared to published fluorescence components in the OpenFluor database (Murphy et al., 2014).

We performed a partial least squares (PLS) analysis to determine which environmental variables best predict adsorption capacity. This multivariate approach allows the multiple explanatory variables (DOM character

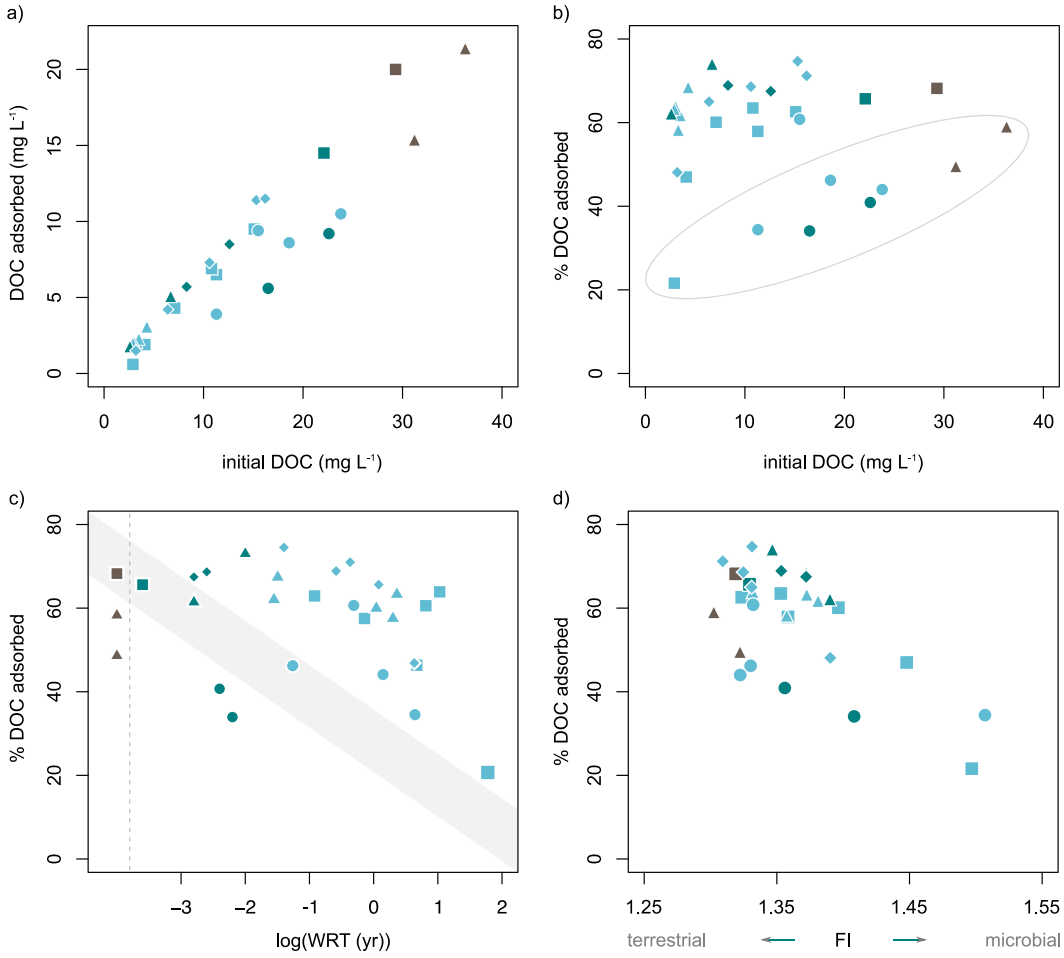

Figure 2. (a) DOC loss resulting from adsorption to clay particles relative to the initial DOC concentration, (b) percentage DOC adsorbed relative to the initial DOC concentration: The encircled samples display a relatively low percentage DOC adsorbed (see section 4), (c) percentage DOC adsorbed relative to the WRT, with the grey shaded area representing the original hypothesized relationship based on the exponential decrease observed for absorbance at 420 nm with increasing WRT (Weyhenmeyer et al., 2012) (note that peat samples have not been assigned a WRT), (d) percentage DOC adsorbed relative to the initial FI of peat (brown), stream (green), and lake (blue) water across four regions of Sweden (Jämtland [triangles], Bergslagen [diamonds], Uppland [circles], and Småland [squares]).

and water chemistry variables) to be teased apart to a certain extent. The PLS algorithm extracts uncorrelated latent components from the data space of the explanatory variables in order to maximally explain the variance in the percentage DOC adsorbed. The model loadings indicate how different explanatory variables load onto latent components. PLS analysis was especially suitable for this data set as it is insensitive to cocorrelations between the predictor variables. Highly skewed predictor variables (skewness >2.0 and/or min/max ratio < 0.1) were log transformed (see Table S3), and the response variable (adsorption capacity, expressed as ΔDOC%) was arcsine transformed to increase model performance. All predictor variables were mean centered and scaled to unit variance prior to analysis. We reduced the number of variables by grouping the cations (Na^+, NH_4^+, K^+, Ca^{2+}, and Mg^{2+}) and anions (F^-, Cl^-, NO_3^-, PO_4^{3-}, and SO_4^{2-}) together, since these were highly cocorrelated. The importance of predictor variables on the model is given by the variable influence on projection (VIP) scores, where VIP scores ≥1 were considered highly influential, 1 > VIP ≥ 0.8 moderately influential and <0.8 less influential. Cross validation was performed to assess the predictive power of the model (Q^2Y) and random permutation testing (100 permutations) of the response variable indicated the statistical significance of the estimated predictive power (Eriksson et al., 2013). PLS modelling was done in SIMCA 15.0 (Umetrics AB, Umeå, Sweden).

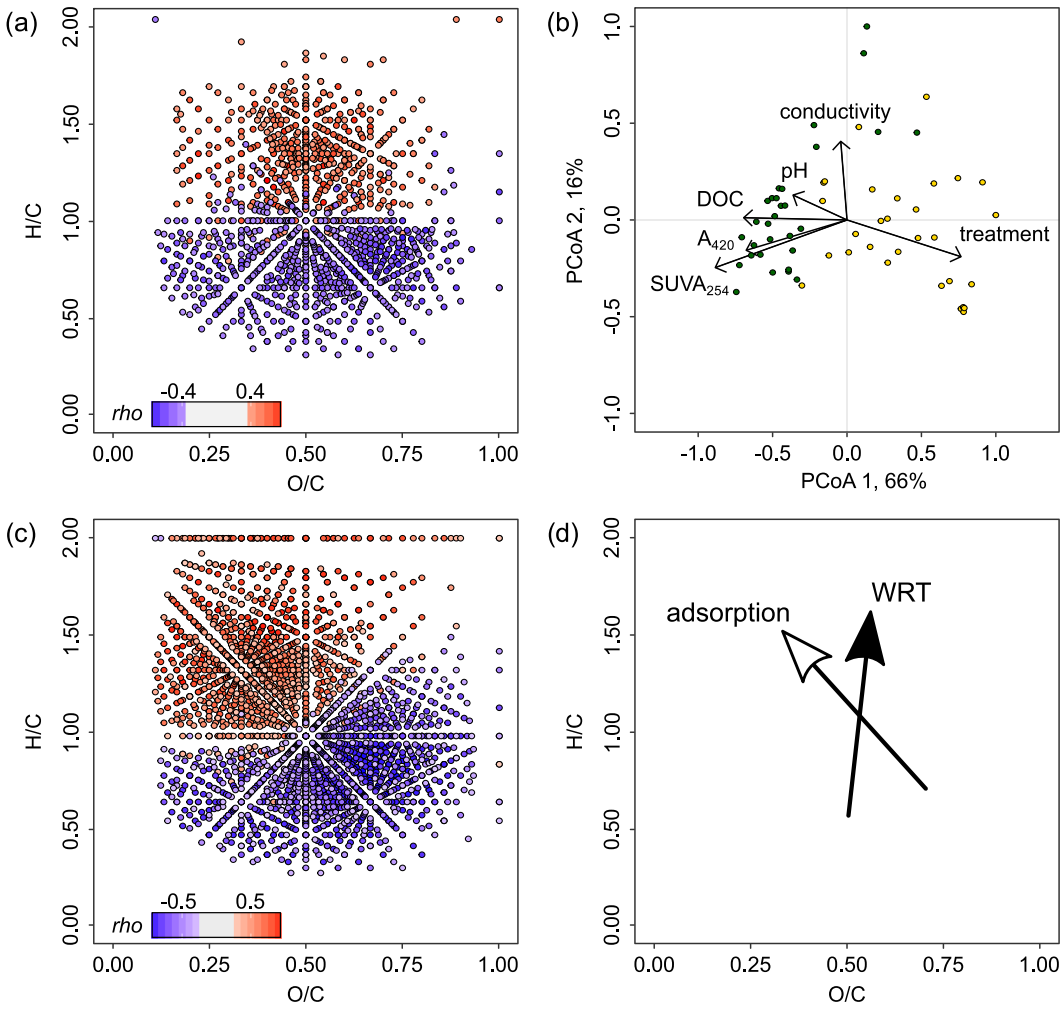

Figure 3. (a) Spearman rank correlation coefficients (correlation limit = 0.362 for 30 samples at $\alpha = 0.05$) of individual molecules with water residence time (WRT), (b) principal coordinate analysis (PCoA) loadings of the samples before (green) and after (yellow) the adsorption treatment with sample characteristics as drivers in the ordination (arrows), (c) Spearman rank correlation coefficients (correlation limit = 0.255 for 60 samples at $\alpha = 0.05$) of individual molecules with PCoA 1, and (d) conceptual representation of the effect of WRT and the adsorption treatment on the DOM pool in van Krevelen space.

3. Results

Losses of DOC due to adsorption to clay particles ranged from 0.6 to 21.2 mg L^{-1} (median = 6.1 mg L^{-1}; Figure 2a). The loss of DOC was in almost all cases accompanied by a decrease in water color as approximated by A_{420} (median: 81%, ranging from a 6% increase to a 100% decrease) and a change in $SUVA_{254}$ (median: 1.3 L mg C^{-1} m^{-1}, ranging from an increase of 0.8 L mg C^{-1} m^{-1} to a decrease of 2.3 L mg C^{-1} m^{-1}) (Table S1). The amount of DOC adsorbed increased linearly with initial DOC concentration of the samples (Siegel repeated medians linear regression, $p < 0.001$; Figure 2a). The relative DOC loss ranged from 22% to 75% (median: 61%) and showed no relationship with the initial DOC concentration (Figure 2b). While we hypothesized that the adsorption capacity of DOC would decrease for sites with longer WRT (grey area in Figure 2c), no clear trend was found across this data set (Figure 2c). Water samples with a higher fluorescence index (FI > 1.4, suggesting more autochthonous DOM) had a lower percentage DOM adsorbed than water samples with a lower fluorescence index (indicating more allochthonous DOM) (Siegel repeated medians linear regression, $p < 0.01$; Figure 2d). The two other fluorescence indices provided complimentary insights, as the percentage of DOM adsorbed decreased with the freshness index (FRESH; Siegel repeated medians linear regression, $p < 0.001$) and increased with increasing humification index (Siegel repeated medians linear regression, $p < 0.01$).

We took an initial step of establishing if DOM composition, as measured by ESI mass spectrometry, shows a predictable pattern across the gradient of WRT. We found that compounds with low H/C are less prevalent at longer WRT, whereas compounds with high H/C are of higher relative importance at longer WRT (Figure 3a). The first component of the PCoA reflected the effect of adsorption on DOM composition, explaining 66% of the variation across the data set and resulted in a separation of the samples before and after adsorption treatment along this first axis (Figure 3b). The second PCoA component explained another 16% of the variation, which appeared to be related to conductivity of the samples. Since "treatment" (i.e., before or after the adsorption treatment) was highly related to the first component in the PCoA analysis, we used the axis of this component as a proxy for the effect of adsorption treatment on DOM in further correlation analysis with the molecular compounds across van Krevelen space (Figure 3c). Compounds with low H/C and high O/C were preferentially adsorbed onto the clay particles, whereas compounds with high H/C and low O/C resisted adsorption and remained in solution. These patterns were also apparent in the weight-averaged values; for the initial samples (before the adsorption treatment), the weighted average of H/C increased at longer WRT (mostly after 1 year), and the adsorption treatment increased the weighted average of H/C for all samples (Figure S2a). The weighted average of O/C was similar across WRT for the initial samples and decreased markedly after the adsorption treatment across the full WRT gradient (Figure S2c). Hence, the DOM composition of the initial samples increased in H/C with increasing WRT but the O/C did not appear to be affected by WRT. There was a clear shift in the elemental composition of extractable and ionizable DOM remaining in solution after the adsorption experiment, with the H/C increasing and O/C simultaneously decreasing due to the loss of compounds with low H/C and high O/C. This pattern can also be observed in the van Krevelen diagrams for all individual samples (Figure S3). WRT and adsorption thus had similar effects on DOM composition with regards to H/C, but different effects on O/C (Figure 3d). The direction of the compositional shift was independent of the initial pH of the samples (Figures S2b and S2d).

PARAFAC of fluorescence EEMs resulted in a validated five-component model (Figure 4a). Comparison to the OpenFluor database showed that all components have been previously identified as DOM components (Tucker congruence coefficient ≥ 0.98 on both the excitation and emission spectra), with components 1–4 being composed of "humic-like" material, whereas component 5 consists of "protein-like" material (OpenFluor references in Table S2). Fluorescence intensity decreased for all components as a result of the adsorption treatment (Wilcoxon signed rank test for paired samples, $p < 0.001$ for C1-4, $p = 0.001$ for C5; Figure 4b). While C1 was dominant in the start samples, all components contributed similarly to the total fluorescence in the end samples (Figure 4c). C1 and C3 were most susceptible to loss by adsorption to clay, with a median decrease of 78% and 74%, respectively, while C5 appeared to be more resistant to adsorption with a median decrease of only 23% (Figure 4d).

A shift in the position of fluorescence peak maxima was observed for post adsorption DOM for two dominant peaks, peak A (Ex_{260}, $Em_{448–480}$) and peak C ($Ex_{320–360}$, $Em_{420–460}$) (Figure 5a). Peak A shifted toward lower emission wavelengths (Wilcoxon signed rank test for paired samples, $p < 0.001$; Figures 5b and 5e), while peak C shifted toward lower emission (Wilcoxon signed rank test for paired samples, $p < 0.001$; Figures 5c and 5f) and higher excitation wavelengths (Wilcoxon signed rank test for paired samples, $p < 0.001$; Figures 5d and 5e). In addition, a decline in the emission wavelength of the maximum of peak A was observed with increasing WRT (Siegel repeated medians linear regression, $p < 0.001$; peats not included in the regression; Figure 5e). The emission wavelength of the maximum of peak C decreased and its excitation wavelength increased with increasing WRT (Siegel repeated medians linear regression, $p < 0.001$ in both cases; peats not included in the regression; Figures 5f and 5g).

The PLS model predicting the percentage of DOC loss extracted one significant component with an R^2Y (variation in the response variable explained) of 0.80. Cross validation showed that the model had a good predictive ability ($Q^2Y = 0.63$). Model validation through a permutation test of the response variable (100 times) showed that the background correlation was small ($R^2Y = 0.04$). The loadings plot (Figures 6) and VIP values (Table S3) identified the freshness index (FRESH), $SUVA_{254}$, 250/365 absorbance ratio (AbsRatio), weight-averaged H/C ratio (HC_{WA}), pH, cations, fluorescence index (FI), TSSs, anions, POC/PN ratio, and conductivity as highly influential explanatory variables of percentage DOC adsorbed. Specifically, percentage DOC adsorbed appeared positively related to $SUVA_{254}$ and POC/PN ratio as these variables are situated on the far right side of the first axis together with percent DOC adsorbed, whereas

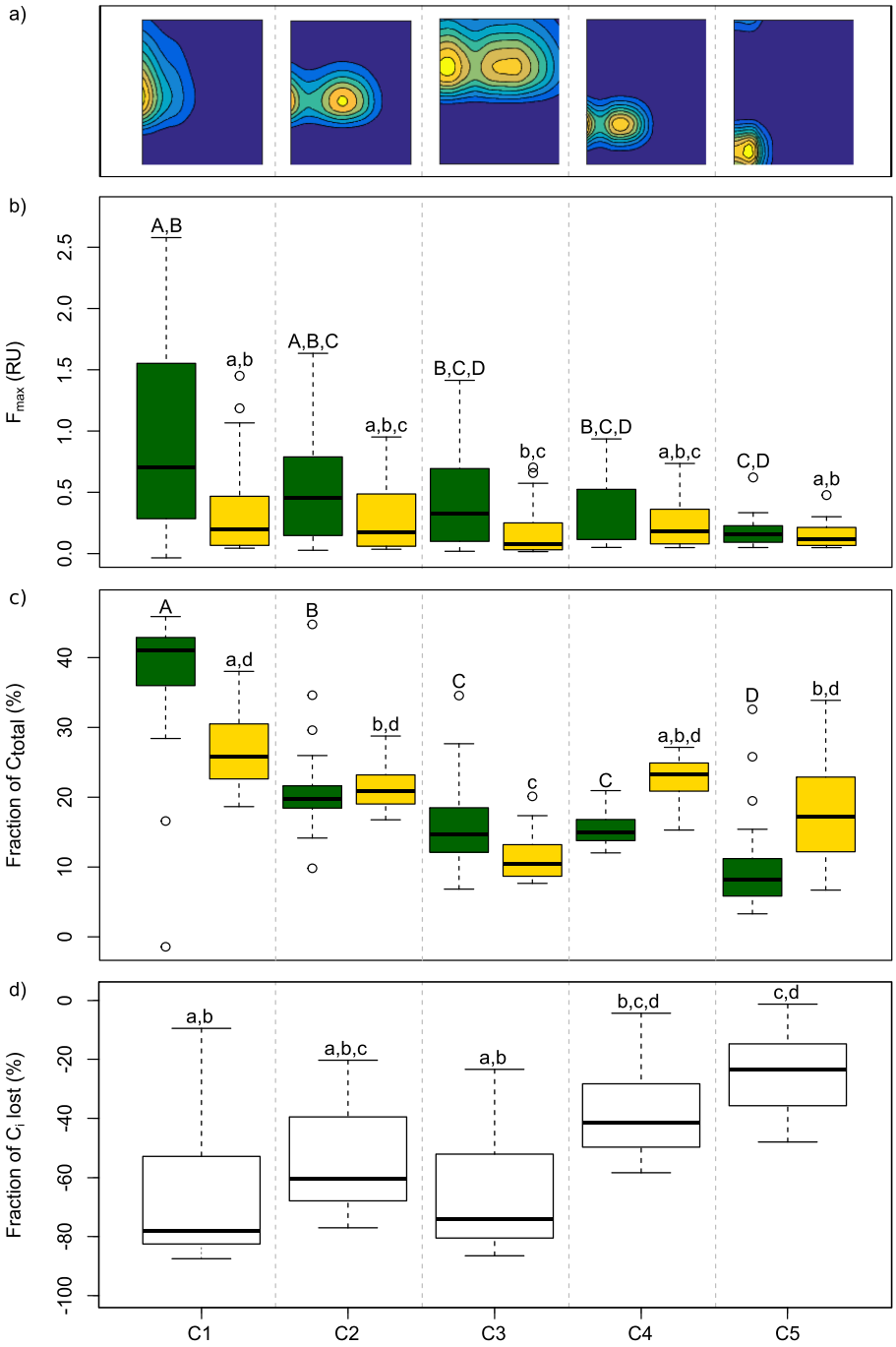

Figure 4. (a) PARAFAC components, (b) the maximum fluorescence intensity (F_{max}) expressed in Raman units for each of the components before (green) and after (yellow) the adsorption treatment, (c) the relative fluorescence intensity of each component expressed as a percentage of the sum of all five component intensities before (green) and after (yellow) the adsorption treatment, respectively, and (d) the fraction of each component lost to adsorption (%). For (b)–(d), box-and-whiskers plots show the median and first and third quartiles with the whiskers set at ±1.5 times the interquartile range and data outside this range given as circles (note that for (d) data outside the range of the box plot are not shown for clarity, as they include extreme outliers). Components that are not significantly different from each other are represented with the same letter above the boxplots.

freshness index, absorbance ratio, HC_{WA}, pH, cations, fluorescence index, TSS, anions, and conductivity were negatively related as these variables are situated to the far left of the first axis, away from percent DOC adsorbed (Figure 6).

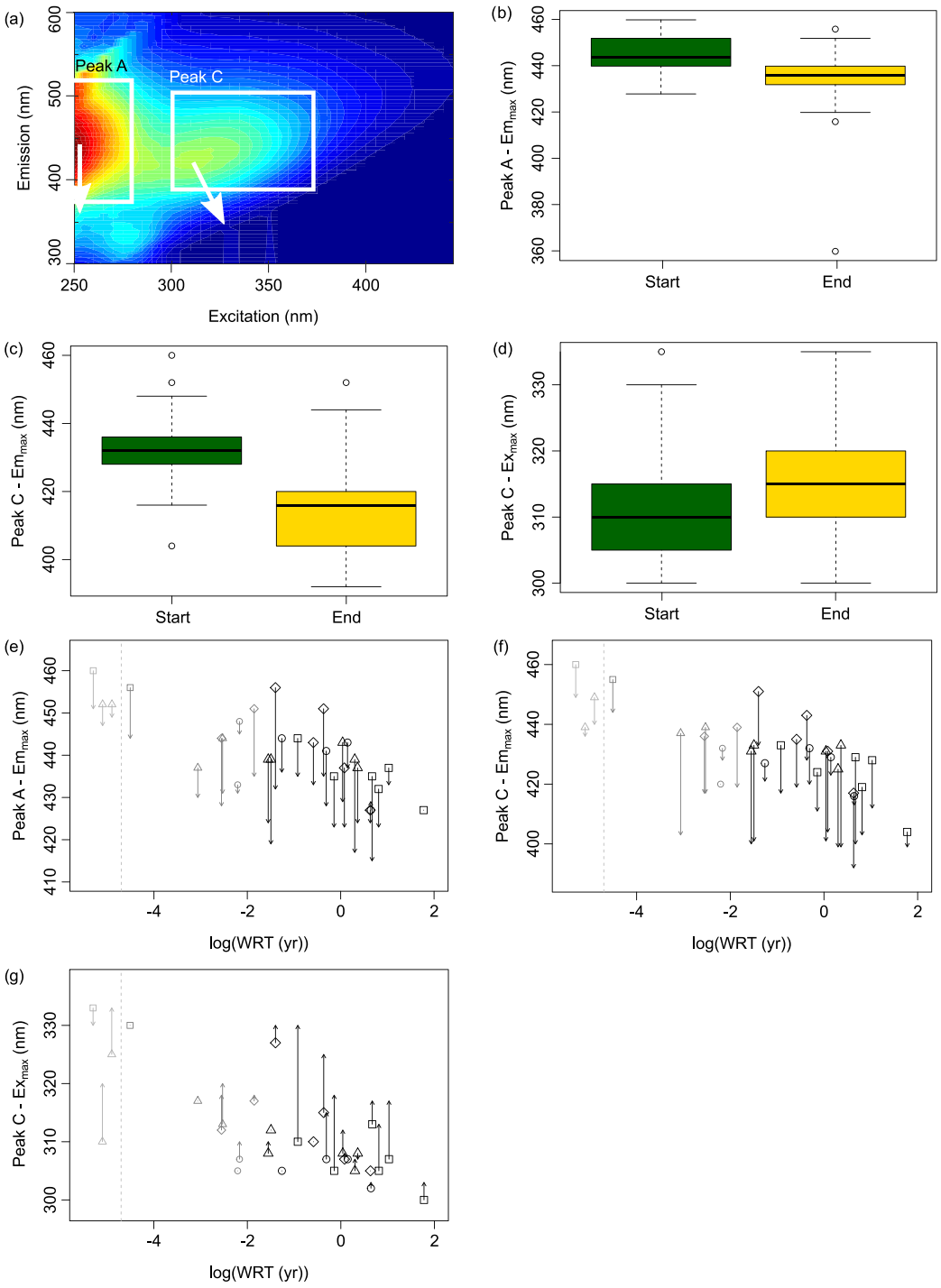

Figure 5. (a) EEM indicating the shift in peak A and peak C (arrows, not to scale) as a result of the adsorption treatment, (b) the maximum emission wavelength at excitation wavelength 250, (c) the maximum emission wavelength at excitation wavelength 300–350, (d) the maximum excitation wavelength at emission wavelength 392–460, (e) the maximum emission wavelength at excitation wavelength 250 relative to the water residence time (WRT), (f) the maximum emission wavelength at excitation wavelength 300–350 relative to the WRT, and (g) the maximum excitation wavelength at emission wavelength 392–346 relative to the WRT. For (b)–(d), the box-and-whiskers plots show the median and first and third quartiles with the whiskers set at ±1.5 times the interquartile range and data outside this range given as circles. For (e)–(g), the length of the arrows denotes the magnitude of the shift from before to after the adsorption treatment for each peat (brown), stream (green), and lake (blue) water across four regions of Sweden (Jämtland [triangles], Bergslagen [diamonds], Uppland [circles], and Småland [squares], so that the arrowhead represents the sample after adsorption, dots indicate no shift. Note that in (e)–(g), peat samples have not been assigned a WRT. All plots are based on triplicates for each sample.

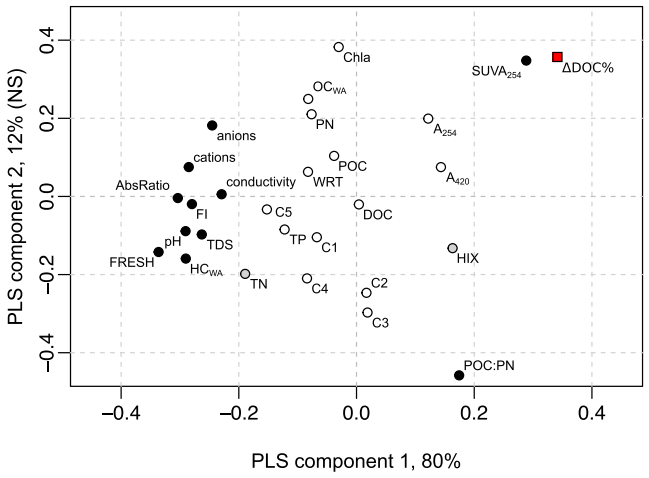

Figure 6. Partial least squares (PLS) loadings plot predicting percentage DOC adsorbed (denoted as ΔDOC%; red square) with water chemistry, molecular, and spectral characteristics as predictor variables. Black circles are highly influential variables (VIP ≥ 1), grey circles are moderately influential (1 > VIP ≥ 0.8), and white circles are less influential variables (VIP < 0.8). Note that PLS component 1 is plotted against nonsignificant (NS) PLS component 2 for clarity.

4. Discussion

4.1. DOM Adsorption to Clay

This study demonstrates that a substantial DOM fraction can be adsorbed onto inorganic particles in a variety of boreal inland waters. Clay was added at a very high concentration (5 g L^{-1}, 2 orders of magnitude higher than typical for waters in the sampled regions), resulting in a very large surface for DOM to interact with. The clay we used is a commercially available reference material, which we chose for its expected high affinity for DOM due to the presence of aluminum and iron oxides (see SI Text S2). The added clay is not a direct representation of mineral surfaces naturally occurring in the sampled watersheds, and it is important to note that the nature of the sorbate, the solution, and the sorbent may affect the selective partitioning of DOM to particle surfaces (e.g., Fleury et al., 2017; Kaiser et al., 1996; Meier et al., 1999). As such, the results observed here apply to this specific combination of mineral particles and water samples (including both the DOM and the solution characteristics). This allows the presented cross-system comparison, but great care should be taken when extrapolating outside the studied region. Instead, the experiment was designed to assess the potential of DOM to adsorb under controlled conditions, following the question: If a suitable inorganic particulate material would be abundant, how would adsorption affect the quantity and quality of DOM? Since adsorption in this experiment greatly exceeds the actual adsorption taking place in boreal inland waters, an increase in mineral erosion in these systems may allow for more adsorption and thereby affect the availability, transport and composition of organic carbon in inland waters.

4.2. Selective DOM Adsorption

Our analyses of DOM quality showed an adsorption-driven DOM fractionation. PARAFAC analysis of the fluorescence spectra showed that long emission wavelength, humic-like components C1 and C3 were preferentially removed and short emission wavelength, protein-like component C5 was most resistant to adsorption (Figure 4). These results show the same pattern as a study where soil and leaf extracts had been adsorbed onto goethite and gibbsite minerals, and the humic-like PARAFAC components decreased with 67%–91%, whereas the protein-like components decreased with only 26%–52% (Banaitis et al., 2006). Long emission wavelength fluorescing DOM compounds are known to be lost due to a variety of processes (e.g., naturally occurring processes on a catchment scale [Kothawala et al., 2014]; photochemical degradation [Du et al., 2016]; $FeCl_3$ coagulation [Lavonen et al., 2015]). The tendency for long emission wavelength FDOM to be lost also manifests itself in the observed shifts in peaks A and C (Figures 5b and 5c). When long emission FDOM components are lost, these common peaks are situated at a lower emission wavelength. This so-called blue shift may be caused by a decrease in the number of aromatic rings, conjugated bonds in a chain structure, and carbonyl, hydroxyl, and amine functional groups (Chen et al., 2003; Senesi, 1990), as well as being indicative of reduced compounds and a decrease in molecular weight (Her et al., 2003). Since these types of compounds are generally adsorbed (see below), the observed blue-shift corresponds with the expected molecular changes in the DOM after adsorption.

Adsorption to mineral surfaces affected the ionizable DOM composition both in the H/C and the O/C dimension (Figures 3c, S2, and S3). Unsaturated compounds (low H/C) are preferentially adsorbed while saturated compounds (high H/C) remain in solution. The same trend has been reported by studies using mass spectrometry to investigate the adsorption of Suwannee River fulvic acid from the International Humic Substances Society on alumina colloids (Galindo & Del Nero, 2014) and soil DOM, International Humic Substances Society Pahokee peat (Chassé et al., 2015) and peat DOM on iron oxyhydroxides (Lv et al., 2016), and soil fulvic acid on alumina colloids (Fleury et al., 2017). Accordingly, studies using other methods than mass spectrometry also found that compounds with low H/C such as polyphenols and aromatics are preferentially adsorbed (Kaiser, 2003; Kaiser et al., 1997; Kalbitz et al., 2005; Kothawala et al.,

2012). This is consistent with the use of coagulation (e.g., to metals) to remove aromatic, high molecular weight compounds during drinking water treatment (Lavonen et al., 2015; Matilainen et al., 2010).

In addition to the shift in H/C with adsorption, we also observed that the adsorbed compounds on average had a higher O/C than the compounds that remained in solution. This is also where WRT and the adsorption treatment diverge in their effect on DOM composition: Whereas unsaturated compounds are generally lost from solution in both processes, even fairly saturated compounds can be adsorbed as long as they have a high O/C (Figures 3c and S3). The observed adsorption of oxygen-rich compounds is in agreement with various other studies, where both highly oxidized aromatics (Coward et al., 2018; Fleury et al., 2017; Galindo & Del Nero, 2014; Lv et al., 2016), and in some cases also oxidized saturated, aliphatic compounds (Galindo & Del Nero, 2014; Avneri-Katz et al., 2017) were preferentially adsorbed. The preferential adsorption of oxygen-rich compounds indicates that the presence of carboxyl and hydroxyl functional groups may be important for adsorptive processes, as these groups allow for ligand exchange with oxide and hydroxide groups at the sorbent's surface (Chassé et al., 2015; Gu et al., 1995; Kaiser, 2003; Kaiser et al., 1997; Kothawala et al., 2012; Lv et al., 2016; Meier et al., 1999; Tipping, 1981b). In addition to O-containing functional groups, N- and S-containing functional groups could also be involved in adsorptive processes (McKnight et al., 1992). We were unable consider these compounds due to the limited resolution of the mass spectrometer, which only permitted assignment of N_1 and S_1 species (Hawkes et al., 2016). The N and S species that were assigned did not show any trend with sorption and were not investigated further.

In summary, mass spectrometry demonstrated the preferential loss of low H/C and high O/C compounds, and a loss of long emission wavelength components was observed with fluorescence analysis. Since long emission wavelength FDOM correlates with unsaturated compounds identified by mass spectrometry (Kellerman et al., 2015; Stubbins et al., 2014), both methods of investigating DOM composition show the same general pattern of selective adsorption of DOM with a terrestrial or allochthonous character. We recognize that both fluorescence and mass spectrometry capture only a fraction, and not necessarily a corresponding fraction (Hawkes et al., 2019; Wünsch et al., 2018), of the total DOM pool, as certain DOM fractions (nonfluorescent DOM and DOM molecules that are excluded in the various steps of the mass spectrometry method, e.g., SPE, ionization; Stubbins et al., 2014; Raeke et al., 2016) are not considered in these analyses. However, both methods have revealed meaningful patterns in DOM compositional data and are in agreement with regard to which types of compounds might be lost after exposure to the clay and which are unaffected.

The change in DOM composition as a result of adsorption to mineral surfaces resembles the change resulting from photodegradation, which also removes colored (Moran et al., 2000), aromatic (Minor et al., 2007), and unsaturated (low H/C) compounds from solution (Stubbins et al., 2010; Ward & Cory, 2016). While there is a considerable overlap between DOM components that are prone to adsorb and those that are photolabile, the two processes have a different effect on the carbon cycle. Photodegradation of DOM may result in mineralization to CO_2 or in partially photooxidized compounds that are generally more bioavailable, thus also contributing to the pool of CO_2 produced in inland waters (Bertilsson & Tranvik, 1998; Cory et al., 2014; Granéli et al., 1996). Adsorption to mineral surfaces, on the other hand, funnels the DOM from solution to the sediment, where, unless mineralized within the sediment, it will be removed from the short-term carbon cycle (Kortelainen et al., 2004; Tranvik et al., 2009). Burial efficiency, defined as the ratio of organic carbon that is ultimately buried to that which reaches the sediment, was found to be between 5% and 62% in a set of boreal lakes (Ferland et al., 2014). However, allochthonous organic matter, which is selectively adsorbed to mineral surfaces, has a higher burial efficiency than autochthonous matter (Gudasz et al., 2012; Sobek et al., 2009), which suggests the potential importance of DOM adsorption to mineral surfaces for a higher burial efficiency.

4.3. DOM Quality and Water Chemistry Predict Percentage DOC Adsorbed

The PLS analysis identified several highly influential predictor variables (Figure 6), which can be divided into two groups: variables related to DOM quality (intrinsic factors) and variables related to water chemistry (extrinsic factors). We will discuss the effect on percentage DOC adsorbed for each group in turn. Highly influential DOM quality variables are the freshness index (FRESH), the 250/365 absorbance ratio (AbsRatio), the specific ultraviolet absorbance at 254 nm ($SUVA_{254}$), weight-averaged H/C ratio (HC_{WA}),

and the FI. $SUVA_{254}$ and absorbance ratio can be seen as "two sides of the same coin," that is, aromaticity and the lack thereof (Peuravuori & Pihlaja, 1997; Weishaar et al., 2003). The weight-averaged H/C ratio, as a measurement of saturation, is closely related to the absorbance ratio, while a low fluorescence index gives an indication of aromaticity (McKnight et al., 2001). Taken together, it follows that high aromaticity is positively related to percentage DOC adsorbed, whereas a high degree of saturation reduces the DOM's susceptibility to adsorb. Similarly, a high freshness ratio (freshly produced, autochthonous DOM) and a high fluorescence index (indicating DOM of microbial origin) are negative predictors of percentage DOC adsorbed. In addition to the DOM quality variables, the POC/PN ratio was positively related to percentage DOC adsorbed. High POC/PN ratio is associated with allochthonous material, whereas a low POC/PN is indicative of autochthonous material (Meyers, 1994). In short, allochthonous OM is a predictor of a high percentage DOC adsorbed, whereas autochthonous OM predicts a low percentage DOC adsorbed.

Water chemistry variables that predict a low percentage DOC adsorbed are high pH, cations, TSS, anions, and conductivity. These variables are likely responsible for the comparatively low percentage DOC absorbed for a subset of samples that stands out in Figures 2a, 2b, and 2d (sites 1, 10, 12, 25, 26, 27, 28, and 30, encircled in Figure 2b), since these samples show a lower percentage of DOC adsorbed than the rest of the samples for any given initial DOC value or fluorescence index. Investigation of the environmental data for these particular sites (Table S1) revealed that these sites (except for peat sites 10 and 12) tend to show a relatively high pH, conductivity, TSS, and divalent cation concentrations (Ca^{2+} and Mg^{2+}), which reflects the effect of regional geology on water chemistry. This is most notable in the Uppland region (samples 25–30) which is characterized by calcareous soils.

The pH dependence of DOM adsorption onto clay surfaces has been observed in other studies (Davis, 1982; Fleury et al., 2017; Gu et al., 1994; Kaiser et al., 1996; Shen, 1999; Tipping, 1981a, 1981b). Both DOM and clay surfaces are generally negatively charged: DOM through the abundance of carboxylic and hydroxylic groups and clay through the presence of (e.g., Al and Fe) oxides and hydroxides in the mineral lattice. At high pH, deprotonation might lead to fewer available adsorption sites on the DOM and negative electrostatic interactions which hinder adsorption. At low pH, DOM is protonated and can thus approach the mineral surface and engage in ligand exchange with −OH groups thereon (Gu et al., 1994; Tipping, 1981a). Protonation does not only allow the DOM to bind to the mineral surfaces but it also decreases repulsion within and between DOM molecules, so that these may be packed more tightly onto the surfaces. In addition, protonation of the DOM decreases its solubility, makes it more hydrophobic, and enhances its affinity for mineral surfaces (Kaiser et al., 1996). Within the pH range of samples included in this data set (pH of 4.4 to 8 immediately before the mineral particles were added), we found that DOM adsorption in samples with higher pH was hindered (Figure S4a), as has been reported before. Previous studies have shown that pH has a substantial impact on DOM adsorption across this range. For example, 50%–60% of lake sediment DOC was adsorbed to aluminum oxide at pH4–6, whereas at pH7–8 only 30%–40% was adsorbed (Davis, 1982), and 80%–90% of peat DOC was adsorbed to soil particles at pH4–5, while only 30%–40% was adsorbed at pH7–8 (Shen, 1999). This suggests that the potential for adsorption was limited for samples at pH7–8, regardless of the DOM composition.

Percentage DOC adsorbed may also be affected by the presence of divalent cations, such as Ca^{2+} and Mg^{2+}. It has been observed that the adsorption of aquatic humic substances on goethite was increased when Ca^{2+} and Mg^{2+} where added to the solution, which has been ascribed to a coadsorption of cations and DOM (Day et al., 1994; Tipping, 1981a). In this so-called cation bridging, divalent cations decrease the electrostatic repulsion between the negatively charged mineral surface and DOM compounds. Other polyvalent cations, such as Fe^{3+} and Al^{3+}, have also been found to affect DOM adsorption to minerals (Theng, 1976), but these were not considered in this study. A high concentration of cations may therefore lead to the expectation of a high percentage DOC adsorbed. In this particular experimental setup, however, samples with naturally high divalent cation concentrations show a lower percentage DOC adsorbed (Figure S4b). We speculate that at least a part of the DOM that is prone to adsorb has reacted with cations in the natural systems and flocculated out of solution. The potential of the DOM from such systems to adsorb has thus already decreased by the time we performed clay additions in the laboratory. This is also illustrated by a study on DOM composition in headwater streams, where oxygen rich, unsaturated compounds were less abundant in sites with

high ionic strength, suggesting that groundwater flow through mineral soils (the source of ionic strength for headwaters) selectively adsorbs these compounds (Hawkes et al., 2018). In addition, the cations and pH were highly correlated in our sampling sites (Figure S4c). This is because the abundance of ions in certain regions leads to a substantial buffering capacity and circumneutral pH, whereas many other boreal systems are acidic. At the same time, cations may have less of an effect at low pH (Meier et al., 1999). At this point, we cannot distinguish between the effects of pH and cations on the percentage DOC adsorbed, although we expect that both played a role.

In the PLS analysis, both cations and anions were identified as negative predictors of percentage DOC adsorbed. We attribute this largely to the inherent covariation between cations and anions, although SO_4^{2-} and PO_4^{3-} tend to compete with DOM for adsorption sites (Chassé & Ohno, 2016; Gobran & Nilsson, 1988; Gu et al., 1994) and thereby lower the potential for DOM to adsorb, while others suggest that at least SO_4^{2-} is easily replaced with DOM (Tipping, 1981a).

4.4. Patterns With WRT

One aim of this study was to investigate whether the adsorption potential of DOM is gradually exhausted with increasing WRT. Previous studies have shown that polyphenolic and aromatic compounds (with low H/C) with a clear terrestrial signature disappear throughout the aquatic continuum with an increasing WRT, while aliphatic and phenolic compounds (high H/C) remain or are produced (Creed et al., 2015; Hutchins et al., 2017; Kellerman et al., 2014; Köhler et al., 2013; Lambert et al., 2016; Weyhenmeyer et al., 2012). Since the polyphenols and aromatics are also the compounds that preferentially adsorb onto mineral surfaces (e.g., Kaiser et al., 1996; Avneri-Katz et al., 2017), we expected that the percentage DOM adsorbed would decrease with increasing WRT, as the terrestrial signature of the DOM decreases. In accordance with this expectation, Luider et al. (2003) found that the susceptibility of DOM to adsorb to ferric hydroxide decreased with increasing WRT, over a gradient of four sites within the same catchment. However, no such direct trend was found across our data set (Figures 2c, S2a, and S2c), spanning multiple catchments. The discrepancy between our results and the study by Luider et al. (2003) can likely be attributed to the difference in spatial scale. Luider et al. (2003) focused on the flow path within one single catchment with relatively homogenous conditions at all sites. Our study covered a broad geographic region with considerable variation in geology and other environmental conditions, which are likely to mask changes within specific flow paths. Still, both studies support a preferential loss of allochthonous DOM during adsorption. Another potential reason is that although our sampling sites cover a large range of WRTs (0–60 years), their distribution is uneven with a bias toward shorter WRT (median = 0.19 years). Nonetheless, the pattern in DOM composition with WRT revealed by mass spectrometry (Figure 3a) is robust, as it also appears in subsets of the data, such as when only peat and stream samples (short WRT), or only lakes are considered. However, there is a portion of high molecular weight (>1 kDa), colored terrestrial matter (absorbance signal at 200–600 nm) that is not detected by ESI mass spectrometry (Hawkes et al., 2019) and the lack of this material may have an important effect on the interpretation of the results. If the colored material is prone to be lost, as has been reported (Weyhenmeyer et al., 2012), then some unknown portion of the DOC loss could be explained by compounds that are not detectable by our ESI-MS technique due to SPE selectivity and the limited analytical window of the Orbitrap MS in terms of ionization and mass range. This would be particularly important in the more colored samples, such as the peats and some of the smaller streams and lakes. However, trends are still observed by ESI-MS, and they correspond to trends in fluorescence peak locations and intensities across this wide geographical region. This shows that the ionizable carboxylic acids are also susceptible to precipitative loss, particularly polycarboxylic acids in lower pH settings. In addition to the compositional shift with WRT, we also observed a so-called blue shift in the location of fluorescence peaks A and C toward lower emissions wavelengths with increasing WRT (Figures 5e–5g). Blue shifts have previously been observed across gradients from freshwater to marine DOM (Boyd & Osburn, 2004; Coble, 1996), where marine samples were more blue shifted than freshwater samples in both their emission and excitation wavelength (Coble, 1996). Similar to a gradient from freshwater to marine systems, the loss of aromatic compounds (Senesi, 1990) and a decrease in molecular weight (Her et al., 2003) also occur within the inland water continuum (Kellerman et al., 2014; Kothawala et al., 2006), which explains why this blue shift could be observed across the inland water continuum studied here.

5. Conclusions and Perspectives

Several previous studies addressed DOM adsorption to different mineral surfaces and across different soil types, typically using a diversity of sorbents, and one or a few sources of DOM (e.g., Kaiser et al., 1996; Luider et al., 2003; Kalbitz et al., 2005; Kothawala et al., 2009). In contrast, here, we used a broad range of DOM sources and one reference material as sorbent. This allowed us to assess the percentage DOM adsorbed to a clay on a landscape scale and along a WRT gradient. Contrary to our hypothesis, the potential for adsorption was not exhausted with increasing WRT. Our results show a high potential for DOM adsorption to mineral surfaces (22%–75% DOC loss), independent of WRTs spanning from less than a day to 60 years. The quantitative loss of DOM to mineral surfaces is manifested as an alteration of molecular composition: Poorly oxidized saturated compounds remain in solution, while unsaturated and highly oxidized compounds are adsorbed. As such, adsorption removes "terrestrial-like" material from the natural pool of DOM, independent of WRT. Furthermore, this study highlights the importance of both DOM quality and water chemistry (most importantly pH and the presence of cations) in predicting the percentage DOC adsorbed at a landscape scale, which may result in regional differences in adsorption potential depending on the bedrock and soil chemistry in the catchment.

The sustained potential for adsorption in this study suggests that sorbents are in short supply in the studied boreal waters relative to the DOM available. It remains to be seen if this is a general property of inland waters. While the presence of mineral surfaces in most freshwater systems is generally low, this is not always the case. Agriculture, forestry, mining practices, and related land use changes may lead to soil erosion and the addition of particles and metals to aquatic systems (Ahtiainen & Huttunen, 2016; Batsaikhan et al., 2017; Nieminen et al., 2010; Van Oost et al., 2007). Tropical systems in particular may experience high inorganic suspended sediment loads (Laraque et al., 2013). Also, glacial meltwater is known to export large amounts of suspended mineral particles (Hallet et al., 1996; Overeem et al., 2017). In situations where such turbid waters mix with water containing terrestrial DOM, hot spots for DOM adsorption to mineral surfaces might exist. We suggest that future studies focus on identifying potential adsorption hot spots along the aquatic continuum which could strongly impact DOM cycling. The identification of such systems could furthermore prompt research into the fate of the adsorbed DOM. In addition, several processes may currently and in the near future add DOM susceptible to adsorption to boreal freshwater systems. First, recovery from acidification increases soil DOM solubility, causing more DOM with a terrestrial signature to enter the aquatic continuum (Ekström et al., 2011; Monteith et al., 2007; SanClements et al., 2012). Second, in places where runoff is predicted to increase with climate change (Schewe et al., 2014), a shorter water residence time may result in a larger proportion of allochthonous DOM (Algesten et al., 2003). This changing carbon pool may as a result be more susceptible to adsorption to mineral particles. In terms of carbon cycling, it will be highly relevant to determine whether the adsorbed DOM is buried into the sediment, desorbed, and/or degraded by microbial and photochemical processes.

Acknowledgments

The study was supported by funds to L. T. and J. B. from the Swedish Research Council (2014-04264 and 2015-4870) and the Knut and Alice Wallenberg Foundation (KAW 2013.0091). K. A. was financially supported by DFG Research Fellowship AT 185/1-1, and N. C. acknowledges the support of the Beatriu de Pinós postdoctoral program (2016-00215) of the Government of Catalonia's Secretariat for Universities and Research of the Ministry of Economy and Knowledge. M. G. and K. E. acknowledge the Malméns Foundation. Sampling was funded by an Olsson Borgh foundation stipend to N. C. Additionally, we thank Christoffer Bergvall and Anna Székely for their laboratory assistance, Anna Freixa for her assistance in the field, and Simone Moras for their help with creating the map. We also thank three anonymous reviewers whose comments helped to improve the manuscript. Additional data are available at the Uppsala University data repository (http://urn.kb.se/resolve?urn=urn:nbn:se:uu:diva-404415).

References

Ahmed, N., Varadachari, C., & Ghosh, K. (2002). Soil clay-humus complexes. II. Bridging cations and DTA studies. *Soil Research*, *40*(4), 705–713. https://doi.org/10.1071/sr01046

Ahtiainen, M., & Huttunen, P. (2016). Long-term effects of forestry managements on water quality and loading in brooks. *Boreal Environ Res*, *4*, 101–114.

Algesten, G., Sobek, S., Bergström, A.-K., Ågren, A., Tranvik, L. J., & Jansson, M. (2003). Role of lakes for organic carbon cycling in the boreal zone. *Global Change Biology*, *10*(1), 141–147. https://doi.org/10.1111/j.1365-2486.2003.00721.x

Amon, R. M. W., & Benner, R. (1996). Bacterial utilization of different size classes of dissolved organic matter. *Limnology and Oceanography*, *41*(1), 41–51. https://doi.org/10.4319/lo.1996.41.1.0041

Attermeyer, K., Catalán, N., Einarsdottir, K., Freixa, A., Groeneveld, M., Hawkes, J. A., & Tranvik, L. J. (2018). Organic carbon processing during transport through boreal inland waters: Particles as important sites. *Journal of Geophysical Research: Biogeosciences*, *123*(8), 2412–2428. https://doi.org/10.1029/2018JG004500

Avneri-Katz, S., Young, R. B., McKenna, A. M., Chen, H., Corilo, Y. E., Polubesova, T., & Chefetz, B. (2017). Adsorptive fractionation of dissolved organic matter (DOM) by mineral soil: Macroscale approach and molecular insight. *Organic Geochemistry*, *103*, 113–124. https://doi.org/10.1016/j.orggeochem.2016.11.004

Banaitis, M. R., Waldrip-Dail, H., Diehl, M. S., Holmes, B. C., Hunt, J. F., Lynch, R. P., & Ohno, T. (2006). Investigating sorption-driven dissolved organic matter fractionation by multidimensional fluorescence spectroscopy and PARAFAC. *Journal of Colloid and Interface Science*, *304*(1), 271–276. https://doi.org/10.1016/j.jcis.2006.07.035

Batsaikhan, B., Kwon, J.-S., Kim, K.-H., Lee, Y.-J., Lee, J.-H., Badarch, M., & Yun, S.-T. (2017). Hydrochemical evaluation of the influences of mining activities on river water chemistry in central northern Mongolia. *Environmental Science and Pollution Research*, *24*(2), 2019–2034. https://doi.org/10.1007/s11356-016-7895-3

Bertilsson, S., & Tranvik, L. J. (1998). Photochemically produced carboxylic acids as substrates for freshwater bacterioplankton. *Limnology and Oceanography*, *43*(5), 885–895. https://doi.org/10.4319/lo.1998.43.5.0885

Boyd, T. J., & Osburn, C. L. (2004). Changes in CDOM fluorescence from allochthonous and autochthonous sources during tidal mixing and bacterial degradation in two coastal estuaries. *Marine Chemistry*, *89*(1), 189–210. https://doi.org/10.1016/j.marchem.2004.02.012

Bro, R. (1997). PARAFAC. Tutorial and applications. *Chemometrics and Intelligent Laboratory Systems*, *38*(2), 149–171. https://doi.org/10.1016/S0169-7439(97)00032-4

Brunberg, A.-K., & Blomqvist, P. (1998). *Vatten i Uppsala län 1997: Beskrivning, utvärdering, åtgärdsförslag*. Uppsala: Upplandsstift.

Catalán, N., Marcé, R., Kothawala, D. N., & Tranvik, L. J. (2016). Organic carbon decomposition rates controlled by water retention time across inland waters. *Nature Geoscience*, *9*(7), 501–504. https://doi.org/10.1038/ngeo2720

Chassé, A. W., & Ohno, T. (2016). Higher molecular mass organic matter molecules compete with orthophosphate for adsorption to iron (oxy)hydroxide. *Environmental Science & Technology*, *50*(14), 7461–7469. https://doi.org/10.1021/acs.est.6b01582

Chassé, A. W., Ohno, T., Higgins, S. R., Amirbahman, A., Yildirim, N., & Parr, T. B. (2015). Chemical force spectroscopy evidence supporting the layer-by-layer model of organic matter binding to iron (oxy)hydroxide mineral surfaces. *Environmental Science & Technology*, *49*(16), 9733–9741. https://doi.org/10.1021/acs.est.5b01877

Chen, J., LeBoeuf, E. J., Dai, S., & Gu, B. (2003). Fluorescence spectroscopic studies of natural organic matter fractions. *Chemosphere*, *50*(5), 639–647. https://doi.org/10.1016/S0045-6535(02)00616-1

Chen, M., & Jaffé, R. (2014). Photo- and bio-reactivity patterns of dissolved organic matter from biomass and soil leachates and surface waters in a subtropical wetland. *Water Research*, *61*, 181–190. https://doi.org/10.1016/j.watres.2014.03.075

Coble, P. G. (1996). Characterization of marine and terrestrial DOM in seawater using excitation-emission matrix spectroscopy. *Marine Chemistry*, *51*(4), 325–346. https://doi.org/10.1016/0304-4203(95)00062-3

Cole, J. J., Prairie, Y. T., Caraco, N. F., McDowell, W. H., Tranvik, L. J., Striegl, R. G., & Melack, J. (2007). Plumbing the global carbon cycle: Integrating inland waters into the terrestrial carbon budget. *Ecosystems*, *10*(1), 172–185. https://doi.org/10.1007/s10021-006-9013-8

Cory, R. M., & McKnight, D. M. (2005). Fluorescence spectroscopy reveals ubiquitous presence of oxidized and reduced quinones in dissolved organic matter. *Environmental Science & Technology*, *39*(21), 8142–8149. https://doi.org/10.1021/es0506962

Cory, R. M., Ward, C. P., Crump, B. C., & Kling, G. W. (2014). Sunlight controls water column processing of carbon in arctic fresh waters. *Science*, *345*(6199), 925–928. https://doi.org/10.1126/science.1253119

Coward, E. K., Ohno, T., & Plante, A. F. (2018). Adsorption and molecular fractionation of dissolved organic matter on iron-bearing mineral matrices of varying crystallinity. *Environmental Science & Technology*, *52*(3), 1036–1044. https://doi.org/10.1021/acs.est.7b04953

Creed, I. F., McKnight, D. M., Pellerin, B. A., Green, M. B., Bergamaschi, B. A., Aiken, G. R., & Stackpoole, S. M. (2015). The river as a chemostat: Fresh perspectives on dissolved organic matter flowing down the river continuum. *Canadian Journal of Fisheries and Aquatic Sciences*, *72*(8), 1272–1285. https://doi.org/10.1139/cjfas-2014-0400

Davis, J. A. (1982). Adsorption of natural dissolved organic matter at the oxide/water interface. *Geochimica et Cosmochimica Acta*, *46*(11), 2381–2393. https://doi.org/10.1016/0016-7037(82)90209-5

Day, G. M., Hart, B. T., McKelvie, I. D., & Beckett, R. (1994). Adsorption of natural organic matter onto goethite. *Colloids and Surfaces A: Physicochemical and Engineering Aspects*, *89*(1), 1–13. https://doi.org/10.1016/0927-7757(94)02855-9

Droppo, I. G., & Ongley, E. D. (1994). Flocculation of suspended sediment in rivers of southeastern Canada. *Water Research*, *28*(8), 1799–1809. https://doi.org/10.1016/0043-1354(94)90253-4

Du, Y., Zhang, Y., Chen, F., Chang, Y., & Liu, Z. (2016). Photochemical reactivities of dissolved organic matter (DOM) in a sub-alpine lake revealed by EEM-PARAFAC: An insight into the fate of allochthonous DOM in alpine lakes affected by climate change. *The Science of the Total Environment*, *568*, 216–225. https://doi.org/10.1016/j.scitotenv.2016.06.036

Ekström, S. M., Kritzberg, E. S., Kleja, D. B., Larsson, N., Nilsson, P. A., Graneli, W., & Bergkvist, B. (2011). Effect of acid deposition on quantity and quality of dissolved organic matter in soil-water. *Environmental Science & Technology*, *45*(11), 4733–4739. https://doi.org/10.1021/es104126f

Eriksson, L., Byrne, T., Johansson, E., Trygg, J., & Vikström, C. (2013). *Multi- and megavariate data analysis basic principles and applications*. Malmö, Sweden: Umetrics Academy.

Evans, C. D., Futter, M. N., Moldan, F., Valinia, S., Frogbrook, Z., & Kothawala, D. N. (2017). Variability in organic carbon reactivity across lake residence time and trophic gradients. *Nature Geoscience*, *10*(11), 832–835. https://doi.org/10.1038/ngeo3051

Fasching, C., Behounek, B., Singer, G. A., & Battin, T. J. (2014). Microbial degradation of terrigenous dissolved organic matter and potential consequences for carbon cycling in brown-water streams. *Scientific Reports*, *4*, 4981. https://doi.org/10.1038/srep04981

Ferland, M., Prairie, Y. T., Teodoru, C., & Giorgio, P. A. (2014). Linking organic carbon sedimentation, burial efficiency, and long-term accumulation in boreal lakes. *Journal of Geophysical Research: Biogeosciences*, *119*(5), 836–847. https://doi.org/10.1002/2013JG002345

Fleury, G., Del Nero, M., & Barillon, R. (2017). Effect of mineral surface properties (alumina, kaolinite) on the sorptive fractionation mechanisms of soil fulvic acids: Molecular-scale ESI-MS studies. *Geochimica et Cosmochimica Acta*, *196*, 1–17. https://doi.org/10.1016/j.gca.2016.09.029

Galindo, C., & Del Nero, M. (2014). Molecular level description of the sorptive fractionation of a fulvic acid on aluminum oxide using electrospray ionization Fourier transform mass spectrometry. *Environmental Science & Technology*, *48*(13), 7401–7408. https://doi.org/10.1021/es501465h

Gobran, G. R., & Nilsson, S. I. (1988). Effects of forest floor leachate on sulfate retention in a spodosol soil. *Journal of Environmental Quality*, *17*(2), 235–238. https://doi.org/10.2134/jeq1988.00472425001700020012x

Gordon, N. D., McMahon, T. A., Finlayson, B. L., Gippel, C. J., & Nathan, R. J. (2004). *Stream hydrology: An introduction for ecologists*, (2nd ed.). Chichester: John Wiley & Sons.

Granéli, W., Lindell, M., & Tranvik, L. (1996). Photo-oxidative production of dissolved inorganic carbon in lakes of different humic content. *Limnology and Oceanography*, *41*(4), 698–706. https://doi.org/10.4319/lo.1996.41.4.0698

Gu, B., Schmitt, J., Chen, Z., Liang, L., & McCarthy, J. F. (1994). Adsorption and desorption of natural organic matter on iron oxide: Mechanisms and models. *Environmental Science & Technology*, *28*(1), 38–46. https://doi.org/10.1021/es00050a007

Gu, B., Schmitt, J., Chen, Z., Liang, L., & McCarthy, J. F. (1995). Adsorption and desorption of different organic matter fractions on iron oxide. *Geochimica et Cosmochimica Acta*, *59*(2), 219–229. https://doi.org/10.1016/0016-7037(94)00282-Q

Gudasz, C., Bastviken, D., Premke, K., Steger, K., & Tranvik, L. J. (2012). Constrained microbial processing of allochthonous organic carbon in boreal lake sediments. *Limnology and Oceanography*, *57*(1), 163–175. https://doi.org/10.4319/lo.2012.57.1.0163

Hallet, B., Hunter, L., & Bogen, J. (1996). Rates of erosion and sediment evacuation by glaciers: A review of field data and their implications. *Global and Planetary Change*, *12*(1), 213–235. https://doi.org/10.1016/0921-8181(95)00021-6

Hawkes, J., Sjöberg, P. J. R., Bergquist, J., & Tranvik, L. (2019). Complexity of dissolved organic matter in the molecular size dimension: Insights from coupled size exclusion chromatography electrospray ionisation mass spectrometry. *Faraday Discussions*. https://doi.org/10.1039/C8FD00222C

Hawkes, J. A., Dittmar, T., Patriarca, C., Tranvik, L., & Bergquist, J. (2016). Evaluation of the orbitrap mass spectrometer for the molecular fingerprinting analysis of natural dissolved organic matter. *Analytical Chemistry*, *88*(15), 7698–7704. https://doi.org/10.1021/acs.analchem.6b01624

Hawkes, J. A., Radoman, N., Bergquist, J., Wallin, M. B., Tranvik, L. J., & Löfgren, S. (2018). Regional diversity of complex dissolved organic matter across forested hemiboreal headwater streams. *Scientific Reports*, *8*(1), 16060. https://doi.org/10.1038/s41598-018-34272-3

Hedges, J. I., & Keil, R. G. (1999). Organic geochemical perspectives on estuarine processes: Sorption reactions and consequences. *Marine Chemistry*, *65*(1), 55–65. https://doi.org/10.1016/S0304-4203(99)00010-9

Her, N., Amy, G., McKnight, D., Sohn, J., & Yoon, Y. (2003). Characterization of DOM as a function of MW by fluorescence EEM and HPLC-SEC using UVA, DOC, and fluorescence detection. *Water Research*, *37*(17), 4295–4303. https://doi.org/10.1016/S0043-1354(03)00317-8

Hosterman, J. W., Flanagan, F. J., Bragg, A., Doughten, M. W., Filby, R. H., Grimm, C., Rogers, N. W. (1987). Mineralogy and instrumental neutron activation analysis of seven National Bureau of Standards and three Instituto de Pesquisas Tecnologicas clay reference samples (USGS Numbered Series No. 957). Retrieved from U.S. Geological Survey, website: http://pubs.er.usgs.gov/publication/cir957

Hunter, W. R., Niederdorfer, R., Gernand, A., Veuger, B., Prommer, J., Mooshammer, M., & Battin, T. J. (2016). Metabolism of mineral-sorbed organic matter and microbial lifestyles in fluvial ecosystems. *Geophysical Research Letters*, *43*(4), 1582–1588. https://doi.org/10.1002/2016GL067719

Hutchins, R. H. S., Aukes, P., Schiff, S. L., Dittmar, T., Prairie, Y. T., & Giorgio, P. A. (2017). The optical, chemical, and molecular dissolved organic matter succession along a boreal soil-stream-river continuum. *Journal of Geophysical Research: Biogeosciences*, *122*(11), 2892–2908. https://doi.org/10.1002/2017JG004094

ISO10260. (1992). Water quality—Measurement of biochemical parameters—Spectrophotometric determination of the chlorophyll-*a* concentration.

Jespersen, A. M., & Christoffersen, K. (1987). Measurements of chlorophyll-*a* from phytoplankton using ethanol as extraction solvent. *Archiv Für Hydrobiologie*, *109*, 445–454.

Kaiser, K. (2003). Sorption of natural organic matter fractions to goethite (α-FeOOH): Effect of chemical composition as revealed by liquid-state 13C NMR and wet-chemical analysis. *Organic Geochemistry*, *34*(11), 1569–1579. https://doi.org/10.1016/S0146-6380(03)00120-7

Kaiser, K., & Guggenberger, G. (2000). The role of DOM sorption to mineral surfaces in the preservation of organic matter in soils. *Organic Geochemistry*, *31*(7–8), 711–725. https://doi.org/10.1016/S0146-6380(00)00046-2

Kaiser, K., Guggenberger, G., Haumaier, L., & Zech, W. (1997). Dissolved organic matter sorption on subsoils and minerals studied by 13C-NMR and DRIFT spectroscopy. *European Journal of Soil Science*, *48*, 301–310. https://doi.org/10.1111/j.1365-2389.1997.tb00550.x

Kaiser, K., Guggenberger, G., & Zech, W. (1996). Sorption of DOM and DOM fractions to forest soils. *Geoderma*, *74*(3-4), 281–303. https://doi.org/10.1016/S0016-7061(96)00071-7

Kalbitz, K., Schwesig, D., Rethemeyer, J., & Matzner, E. (2005). Stabilization of dissolved organic matter by sorption to the mineral soil. *Soil Biology and Biochemistry*, *37*(7), 1319–1331. https://doi.org/10.1016/j.soilbio.2004.11.028

Keil, R. G., Montluçon, D. B., Prahl, F. G., & Hedges, J. I. (1994). Sorptive preservation of labile organic matter in marine sediments. *Nature*, *370*(6490), 549–552. https://doi.org/10.1038/370549a0

Kellerman, A. M., Dittmar, T., Kothawala, D. N., & Tranvik, L. J. (2014). Chemodiversity of dissolved organic matter in lakes driven by climate and hydrology. *Nature Communications*, 5. https://doi.org/10.1038/ncomms4804

Kellerman, A. M., Kothawala, D. N., Dittmar, T., & Tranvik, L. J. (2015). Persistence of dissolved organic matter in lakes related to its molecular characteristics. *Nature Geoscience*, *8*(6), 454–457. https://doi.org/10.1038/ngeo2440

Kleber, M., Eusterhues, K., Keiluweit, M., Mikutta, C., Mikutta, R., & Nico, P. S. (2015). Chapter one—Mineral-organic associations: Formation, properties, and relevance in soil environments. *Advances in Agronomy*, (Vol. 130, pp. 1–140). Elsevier. https://doi.org/10.1016/bs.agron.2014.10.005

Kleber, M., & Johnson, M. G. (2010). Advances in understanding the molecular structure of soil organic matter. In *Advances in Agronomy* (Vol. 106, pp. 77–142). Elsevier. https://doi.org/10.1016/S0065-2113(10)06003-7

Koehler, B., Landelius, T., Weyhenmeyer, G. A., Machida, N., & Tranvik, L. J. (2014). Sunlight-induced carbon dioxide emissions from inland waters. *Global Biogeochemical Cycles*, *28*(7), 696–711. https://doi.org/10.1002/2014GB004850

Köhler, S. J., Kothawala, D., Futter, M. N., Liungman, O., & Tranvik, L. (2013). In-lake processes offset increased terrestrial inputs of dissolved organic carbon and color to lakes. *PLoS ONE*, *8*(8), e70598. https://doi.org/10.1371/journal.pone.0070598

Kortelainen, P., Pajunen, H., Rantakari, M., & Saarnisto, M. (2004). A large carbon pool and small sink in boreal Holocene lake sediments. *Global Change Biology*, *10*(10), 1648–1653. https://doi.org/10.1111/j.1365-2486.2004.00848.x

Kothawala, D. N., Evans, R. D., & Dillon, P. J. (2006). Changes in the molecular weight distribution of dissolved organic carbon within a Precambrian shield stream. *Water Resources Research*, *42*(5). https://doi.org/10.1029/2005WR004441

Kothawala, D. N., Moore, T. R., & Hendershot, W.H. (2009). Soil Properties Controlling the Adsorption of Dissolved Organic Carbon to Mineral Soils. *Soil Science Society of America Journal*, *73*(6), 1831–1842. https://doi.org/10.2136/sssaj2008.0254

Kothawala, D. N., Murphy, K. R., Stedmon, C. A., Weyhenmeyer, G. A., & Tranvik, L. J. (2013). Inner filter correction of dissolved organic matter fluorescence: Correction of inner filter effects. *Limnology and Oceanography: Methods*, *11*(12), 616–630. https://doi.org/10.4319/lom.2013.11.616

Kothawala, D. N., Roehm, C., Blodau, C., & Moore, T. R. (2012). Selective adsorption of dissolved organic matter to mineral soils. *Geoderma*, *189–190*, 334–342. https://doi.org/10.1016/j.geoderma.2012.07.001

Kothawala, D. N., Stedmon, C. A., Müller, R. A., Weyhenmeyer, G. A., Köhler, S. J., & Tranvik, L. J. (2014). Controls of dissolved organic matter quality: evidence from a large-scale boreal lake survey. *Global Change Biology*, *20*(4), 1101–1114. https://doi.org/10.1111/gcb.12488

Lambert, T., Bouillon, S., Darchambeau, F., Massicotte, P., & Borges, A. V. (2016). Shift in the chemical composition of dissolved organic matter in the Congo River network. *Biogeosciences*, *13*(18), 5405–5420. https://doi.org/10.5194/bg-13-5405-2016

Laraque, A., Castellanos, B., Steiger, J., Lòpez, J. L., Pandi, A., Rodriguez, M., & Lagane, C. (2013). A comparison of the suspended and dissolved matter dynamics of two large inter-tropical rivers draining into the Atlantic Ocean: The Congo and the Orinoco. *Hydrological Processes*, *27*(15), 2153–2170. https://doi.org/10.1002/hyp.9776

Lavonen, E. E., Kothawala, D. N., Tranvik, L. J., Gonsior, M., Schmitt-Kopplin, P., & Köhler, S. J. (2015). Tracking changes in the optical properties and molecular composition of dissolved organic matter during drinking water production. *Water Research*, *85*, 286–294. https://doi.org/10.1016/j.watres.2015.08.024

Lawaetz, A. J., & Stedmon, C. A. (2009). Fluorescence intensity calibration using the Raman scatter peak of water. *Applied Spectroscopy*, *63*(8), 936–940. https://doi.org/10.1366/000370209788964548

Lindell, M. J., Bremle, G., Broberg, O., & Larsson, P. (2001). Monitoring of persistent organic pollutants (POPs): Examples from Lake Vättern, Sweden. *Ambio*, *30*(8), 545–551. https://doi.org/10.1579/0044-7447-30.8.545

Luider, C., Petticrew, E., & Curtis, P. J. (2003). Scavenging of dissolved organic matter (DOM) by amorphous iron hydroxide particles Fe (OH)3(s). *Hydrobiologia*, *494*(1), 37–41. https://doi.org/10.1023/A:1025473122729

Lv, J., Zhang, S., Wang, S., Luo, L., Cao, D., & Christie, P. (2016). Molecular-scale investigation with ESI-FT-ICR-MS on fractionation of dissolved organic matter induced by adsorption on iron oxyhydroxides. *Environmental Science & Technology*, *50*(5), 2328–2336. https://doi.org/10.1021/acs.est.5b04996

Matilainen, A., Vepsäläinen, M., & Sillanpää, M. (2010). Natural organic matter removal by coagulation during drinking water treatment: A review. *Advances in Colloid and Interface Science*, *159*(2), 189–197. https://doi.org/10.1016/j.cis.2010.06.007

Mayer, L. M. (1994a). Relationships between mineral surfaces and organic carbon concentrations in soils and sediments. *Chemical Geology*, *114*(3), 347–363. https://doi.org/10.1016/0009-2541(94)90063-9

Mayer, L. M. (1994b). Surface area control of organic carbon accumulation in continental shelf sediments. *Geochimica et Cosmochimica Acta*, *58*(4), 1271–1284. https://doi.org/10.1016/0016-7037(94)90381-6

McKnight, D. M., Bencala, K. E., Zellweger, G. W., Aiken, G. R., Feder, G. L., & Thorn, K. A. (1992). Sorption of dissolved organic carbon by hydrous aluminum and iron oxides occurring at the confluence of Deer Creek with the Snake River, Summit County, Colorado. *Environmental Science & Technology*, *26*(7), 1388–1396. https://doi.org/10.1021/es00031a017

McKnight, D. M., Boyer, E. W., Westerhoff, P. K., Doran, P. T., Kulbe, T., & Andersen, D. T. (2001). Spectrofluorometric characterization of dissolved organic matter for indication of precursor organic material and aromaticity. *Limnology and Oceanography*, *46*(1), 38–48. https://doi.org/10.4319/lo.2001.46.1.0038

Meier, M., Namjesnik-Dejanovic, K., Maurice, P. A., Chin, Y.-P., & Aiken, G. R. (1999). Fractionation of aquatic natural organic matter upon sorption to goethite and kaolinite. *Chemical Geology*, *157*(3–4), 275–284. https://doi.org/10.1016/S0009-2541(99)00006-6

Menzel, D. W., & Corwin, N. (1965). The measurement of total phosphorus in seawater based on the liberation of organically bound fractions by persulfate oxidation1. *Limnology and Oceanography*, *10*(2), 280–282. https://doi.org/10.4319/lo.1965.10.2.0280

Meyers, P. A. (1994). Preservation of elemental and isotopic source identification of sedimentary organic matter. *Chemical Geology*, *114*(3), 289–302. https://doi.org/10.1016/0009-2541(94)90059-0

Minor, E. C., Dalzell, B. J., Stubbins, A., & Mopper, K. (2007). Evaluating the photoalteration of estuarine dissolved organic matter using direct temperature-resolved mass spectrometry and UV-visible spectroscopy. *Aquatic Sciences*, *69*(4), 440–455. https://doi.org/10.1007/s00027-007-0897-y

Monsen, N. E., Cloern, J. E., Lucas, L. V., & Monismith, S. G. (2002). A comment on the use of flushing time, residence time, and age as transport time scales. *Limnology and Oceanography*, *47*(5), 1545–1553. https://doi.org/10.4319/lo.2002.47.5.1545

Monteith, D. T., Stoddard, J. L., Evans, C. D., de Wit, H. A., Forsius, M., Høgåsen, T., & Vesely, J. (2007). Dissolved organic carbon trends resulting from changes in atmospheric deposition chemistry. *Nature*, *450*(7169), 537–540. https://doi.org/10.1038/nature06316

Moran, M. A., Sheldon, W. M., & Zepp, R. G. (2000). Carbon loss and optical property changes during long-term photochemical and biological degradation of estuarine dissolved organic matter. *Limnology and Oceanography*, *45*(6), 1254–1264. https://doi.org/10.4319/lo.2000.45.6.1254

Murphy, K. R., Butler, K. D., Spencer, R. G. M., Stedmon, C. A., Boehme, J. R., & Aiken, G. R. (2010). Measurement of dissolved organic matter fluorescence in aquatic environments: An interlaboratory comparison. *Environmental Science & Technology*, *44*(24), 9405–9412. https://doi.org/10.1021/es102362t

Murphy, K. R., Stedmon, C. A., Graeber, D., & Bro, R. (2013). Fluorescence spectroscopy and multi-way techniques. *PARAFAC. Analytical Methods*, *5*(23), 6557–6566. https://doi.org/10.1039/C3AY41160E

Murphy, K. R., Stedmon, C. A., Wenig, P., & Bro, R. (2014). OpenFluor—An online spectral library of auto-fluorescence by organic compounds in the environment. *Analytical Methods*, *6*(3), 658–661. https://doi.org/10.1039/C3AY41935E

Nieminen, M., Ahti, E., Koivusalo, H., Mattson, T., Sarkkola, S., & Lauren, A. (2010). Export of suspended solids and dissolved elements from peatland areas after ditch network maintenance in south-central Finland. *Silva Fennica*, *44*(1), 39–49. https://doi.org/10.14214/sf.161

Nieuwenhuize, J., Maas, Y. E. M., & Middelburg, J. J. (1994). Rapid analysis of organic carbon and nitrogen in particulate materials. *Marine Chemistry*, *45*(3), 217–224. https://doi.org/10.1016/0304-4203(94)90005-1

Nisell, J., Lindsjö, A., & Temnerud, J. (2007). *Rikstäckande virtuellt vattendrags nätverk för flödesbaserad modellering VIVAN. (No. 2007:17)*. Uppsala: SLU Institutionen för Miljöanalys.

Ohno, T. (2002). Fluorescence inner-filtering correction for determining the humification index of dissolved organic matter. *Environmental Science & Technology*, *36*(4), 742–746. https://doi.org/10.1021/es0155276

Overeem, I., Hudson, B. D., Syvitski, J. P. M., Mikkelsen, A. B., Hasholt, B., van den Broeke, M. R., & Morlighem, M. (2017). Substantial export of suspended sediment to the global oceans from glacial erosion in Greenland. *Nature Geoscience*, *10*(11), ngeo3046. https://doi.org/10.1038/ngeo3046

Parlanti, E., Wörz, K., Geoffroy, L., & Lamotte, M. (2000). Dissolved organic matter fluorescence spectroscopy as a tool to estimate biological activity in a coastal zone submitted to anthropogenic inputs. *Organic Geochemistry*, *31*(12), 1765–1781. https://doi.org/10.1016/S0146-6380(00)00124-8

Peuravuori, J., & Pihlaja, K. (1997). Molecular size distribution and spectroscopic properties of aquatic humic substances. *Analytica Chimica Acta*, *337*(2), 133–149. https://doi.org/10.1016/S0003-2670(96)00412-6

Raeke, J., Lechtenfeld, O. J., Wagner, M., Herzsprung, P., & Reemtsma, T. (2016). Selectivity of solid phase extraction of freshwater dissolved organic matter and its effect on ultrahigh resolution mass spectra. *Environmental Science: Processes & Impacts*, *18*(7), 918–927. https://doi.org/10.1039/C6EM00200E

Raymond, P. A., Saiers, J. E., & Sobczak, W. V. (2016). Hydrological and biogeochemical controls on watershed dissolved organic matter transport: pulse-shunt concept. *Ecology*, 97. https://doi.org/10.1890/14-1684.1

SanClements, M. D., Oelsner, G. P., McKnight, D. M., Stoddard, J. L., & Nelson, S. J. (2012). New insights into the source of decadal increases of dissolved organic matter in acid-sensitive lakes of the northeastern United States. *Environmental Science & Technology*, *46*(6), 3212–3219. https://doi.org/10.1021/es204321x

Schewe, J., Heinke, J., Gerten, D., Haddeland, I., Arnell, N. W., Clark, D. B., & Kabat, P. (2014). Multimodel assessment of water scarcity under climate change. *Proceedings of the National Academy of Sciences*, *111*(9), 3245–3250. https://doi.org/10.1073/pnas.1222460110

Seidel, M., Yager, P. L., Ward, N. D., Carpenter, E. J., Gomes, H. R., Krusche, A. V., et al. (2015). Molecular-level changes of dissolved organic matter along the Amazon River-to-ocean continuum. *Marine Chemistry, 177, Part*, *2*, 218–231. https://doi.org/10.1016/j.marchem.2015.06.019

Senesi, N. (1990). Molecular and quantitative aspects of the chemistry of fulvic acid and its interactions with metal ions and organic chemicals: Part II. The fluorescence spectroscopy approach. *Analytica Chimica Acta*, *232*, 77–106. https://doi.org/10.1016/S0003-2670(00)81226-X

Shen, Y.-H. (1999). Sorption of natural dissolved organic matter on soil. *Chemosphere*, *38*(7), 1505–1515. https://doi.org/10.1016/S0045-6535(98)00371-3

Siegel, A. F. (1982). Robust regression using repeated medians. *Biometrika*, *69*(1), 242–244. https://doi.org/10.1093/biomet/69.1.242

Sobek, S., Durisch-Kaiser, E., Zurbrügg, R., Wongfun, N., Wessels, M., Pasche, N., & Wehrli, B. (2009). Organic carbon burial efficiency in lake sediments controlled by oxygen exposure time and sediment source. *Limnology and Oceanography*, *54*(6), 2243–2254. https://doi.org/10.4319/lo.2009.54.6.2243

Sobek, S., Tranvik, L. J., Prairie, Y. T., Kortelainen, P., & Cole, J. J. (2007). Patterns and regulation of dissolved organic carbon: An analysis of 7,500 widely distributed lakes. *Limnology and Oceanography*, *52*(3), 1208–1219. https://doi.org/10.4319/lo.2007.52.3.1208

Sollins, P., Homann, P., & Caldwell, B. A. (1996). Stabilization and destabilization of soil organic matter: Mechanisms and controls. *Geoderma*, *74*(1–2), 65–105. https://doi.org/10.1016/S0016-7061(96)00036-5

Stubbins, A., Lapierre, J.-F., Berggren, M., Prairie, Y. T., Dittmar, T., & del Giorgio, P. A. (2014). What's in an EEM? Molecular signatures associated with dissolved organic fluorescence in boreal Canada. *Environmental Science & Technology*, *48*(18), 10598–10606. https://doi.org/10.1021/es502086e

Stubbins, A., Spencer, R. G. M., Chen, H., Hatcher, P. G., Mopper, K., Hernes, P. J., & Six, J. (2010). Illuminated darkness: Molecular signatures of Congo River dissolved organic matter and its photochemical alteration as revealed by ultrahigh precision mass spectrometry. *Limnology and Oceanography*, *55*(4), 1467–1477. https://doi.org/10.4319/lo.2010.55.4.1467

Syvitski, J. P. M., Vörösmarty, C. J., Kettner, A. J., & Green, P. (2005). Impact of humans on the flux of terrestrial sediment to the global coastal ocean. *Science*, *308*(5720), 376–380. https://doi.org/10.1126/science.1109454

Theng, B. K. G. (1976). Interactions between montmorillonite and fulvic acid. *Geoderma*, *15*(3), 243–251. https://doi.org/10.1016/0016-7061(76)90078-1

Tipping, E. (1981a). Adsorption by goethite (α-FeOOH) of humic substances from three different lakes. *Chemical Geology*, *33*(1), 81–89. https://doi.org/10.1016/0009-2541(81)90086-3

Tipping, E. (1981b). The adsorption of aquatic humic substances by iron oxides. *Geochimica et Cosmochimica Acta*, *45*, 191–199. https://doi.org/10.1016/0016-7037(81)90162-9

Tranvik, L. J., Downing, J. A., Cotner, J. B., Loiselle, S. A., Striegl, R. G., Ballatore, T. J., & others (2009). Lakes and reservoirs as regulators of carbon cycling and climate. *Limnology and Oceanography*, *54*(6part2), 2298–2314. https://doi.org/10.4319/lo.2009.54.6_part_2.2298

Tremblay, L., & Gagné, J.-P. (2009). Organic matter distribution and reactivity in the waters of a large estuarine system. *Marine Chemistry*, *116*(1), 1–12. https://doi.org/10.1016/j.marchem.2009.09.006

Uher, G., Hughes, C., Henry, G., & Upstill-Goddard, R. C. (2001). Non-conservative mixing behavior of colored dissolved organic matter in a humic-rich, turbid estuary. *Geophysical Research Letters*, *28*(17), 3309–3312. https://doi.org/10.1029/2000GL012509

Van Oost, K., Quine, T. A., Govers, G., Gryze, S. D., Six, J., Harden, J. W., & Merckx, R. (2007). The impact of agricultural soil erosion on the global carbon cycle. *Science*, *318*(5850), 626–629. https://doi.org/10.1126/science.1145724

Von Wachenfeldt, E., & Tranvik, L. J. (2008). Sedimentation in boreal lakes—The role of flocculation of allochthonous dissolved organic matter in the water column. *Ecosystems*, *11*(5), 803–814. https://doi.org/10.1007/s10021-008-9162-z

Walling, D. E., & Fang, D. (2003). Recent trends in the suspended sediment loads of the world's rivers. *Global and Planetary Change*, *39*(1), 111–126. https://doi.org/10.1016/S0921-8181(03)00020-1

Ward, C. P., & Cory, R. M. (2016). Complete and partial photo-oxidation of dissolved organic matter draining permafrost soils. *Environmental Science & Technology*, *50*(7), 3545–3553. https://doi.org/10.1021/acs.est.5b05354

Weishaar, J. L., Aiken, G. R., Bergamaschi, B. A., Fram, M. S., Fujii, R., & Mopper, K. (2003). Evaluation of specific ultraviolet absorbance as an indicator of the chemical composition and reactivity of dissolved organic carbon. *Environmental Science & Technology*, *37*(20), 4702–4708. https://doi.org/10.1021/es030360x

Weyhenmeyer, G. A., Fröberg, M., Karltun, E., Khalili, M., Kothawala, D., Temnerud, J., & Tranvik, L. J. (2012). Selective decay of terrestrial organic carbon during transport from land to sea. *Global Change Biology*, *18*(1), 349–355. https://doi.org/10.1111/j.1365-2486.2011.02544.x

Wünsch, U. J., Geuer, J. K., Lechtenfeld, O. J., Koch, B. P., Murphy, K. R., & Stedmon, C. A. (2018). Quantifying the impact of solid-phase extraction on chromophoric dissolved organic matter composition. *Marine Chemistry*.. https://doi.org/10.1016/j.marchem.2018.08.010

Yoon, T. H., Johnson, S. B., Musgrave, C. B., & Brown, G. E. (2004). Adsorption of organic matter at mineral/water interfaces: I. ATR-FTIR spectroscopic and quantum chemical study of oxalate adsorbed at boehmite/water and corundum/water interfaces. *Geochimica et Cosmochimica Acta*, *68*(22), 4505–4518. https://doi.org/10.1016/j.gca.2004.04.025

References From the Supporting Information

Cawley, K. M., Butler, K. D., Aiken, G. R., Larsen, L. G., Huntington, T. G., & McKnight, D. M. (2012). Identifying fluorescent pulp mill effluent in the Gulf of Maine and its watershed. *Marine Pollution Bulletin*, *64*(8), 1678–1687. https://doi.org/10.1016/j.marpolbul.2012.05.040

Graeber, D., Gelbrecht, J., Pusch, M. T., Anlanger, C., & von Schiller, D. (2012). Agriculture has changed the amount and composition of dissolved organic matter in Central European headwater streams. *Science of The Total Environment*, *438*, 435–446. https://doi.org/10.1016/j.scitotenv.2012.08.087

Murphy, K.R., Bro, R., & Stedmon, C. A. (2014). Chemometric analysis of organic matter fluorescence. In P. G. Coble, J. Lead, A. Baker, D. M. Reynolds, & R. G. M. E. Spencer (Eds.), *Aquatic Organic Matter Fluorescence* (pp. 339–375). New York: Cambridge University Press.

Yamashita, Y., Scinto, L. J., Maie, N., & Jaffé, R. (2010). Dissolved organic matter characteristics across a subtropical wetland's landscape: Application of optical properties in the assessment of environmental dynamics. *Ecosystems*, *13*(7), 1006–1019. https://doi.org/10.1007/s10021-010-9370-1

Yamashita, Y., Maie, N., Briceño, H., & Jaffé, R. (2010). Optical characterization of dissolved organic matter in tropical rivers of the Guayana Shield, Venezuela. *Journal of Geophysical Research: Biogeosciences*, *115*(G1). https://doi.org/10.1029/2009JG000987

Shutova, Y., Baker, A., Bridgeman, J., & Henderson, R. K. (2014). Spectroscopic characterisation of dissolved organic matter changes in drinking watertreatment: From PARAFAC analysis to online monitoring wavelengths. *Water Research*, *54*, 159–169. https://doi.org/10.1016/j.watres.2014.01.053

Peleato, N. M., Sidhu, B. S., Legge, R. L., & Andrews, R. C. (2017). Investigation of ozone and peroxone impacts on natural organic matter character andbiofiltration performance using fluorescence spectroscopy. *Chemosphere*, *172*, 225–233. https://doi.org/10.1016/j.chemosphere.2016.12.118

Peleato, N. M., McKie, M., Taylor-Edmonds, L., Andrews, S. A., Legge, R. L., & Andrews, R. C. (2016). Fluorescence spectroscopy for monitoring reduction of natural organic matter and halogenated furanone precursors by biofiltration. *Chemosphere*, *153*, 155–161. https://doi.org/10.1016/j.chemosphere.2016.03.018